2016

Directed differentiation of human induced pluripotent stem cells into endothelial cells

BOSTON UNIVERSITY

HENRY M. GOLDMAN SCHOOL OF DENTAL MEDICINE

DISSERTATION

DIRECTED DIFFERENTIATION OF HUMAN INDUCED PLURIPOTENT STEM CELLS INTO ENDOTHELIAL CELLS

by

MOHMAED JAMAL AHMED

D.D.S., Ajman University, 2006

C.A.G.S., Boston University Institute for Dental Research and Education – Dubai, 2011

M.S.D., Boston University Institute for Dental Research and Education – Dubai, 2011

Submitted in partial fulfillment of the requirements for the degree of

Doctor of Science in Dentistry

In the department of Endodontics

2016

Approved by

First Reader _____

Darrell N. Kotton, M.D.

Seldin Professor of Medicine

Director, Center for Regenerative Medicine, Boston University and Boston Medical Center

Second Reader _____

Andrew Wilson, M.D.

Assistant Professor of Medicine and Pathology

Director, The Alpha-1 Center

Boston University School of Medicine

DIRECTED DIFFERENTIATION OF HUMAN INDUCED PLURIPOTENT STEM CELLS INTO ENDOTHELIAL CELLS

MOHMAED JAMAL AHMED

Boston University, Henry M. Goldman School of Dental Medicine, 2016

Major Professor: Darrell N. Kotton, M.D., Seldin Professor of Medicine, Director, Center for Regenerative Medicine, Boston University and Boston Medical Center

ABSTRACT

Endothelial cells (ECs) are part of almost every human organ, and disturbance in their function can cause several human diseases such as pulmonary arterial hypertension. We sought to develop an in vitro model to derive ECs from human induced pluripotent stem cells (hiPSCs) in an effort to develop future regenerative therapies or disease models. By stimulating signaling pathways gleaned from prior studies of the early embryonic development of endothelial cells and their precursor germlayer, mesoderm, hiPSCs were differentiated in vitro using a media containing 10ng/ml of Activin, FGF2, VEGF and BMP4 to induce mesoderm over 4 days, followed by VEGF and FGF2 to subsequently specify ECs. By day 12, putative endothelial cells identified by the co-expression of CD31, CD144 and KDR, emerged and could be sorted and re-plated in endothelial maintenance media for expansion over several passages. Time series characterization of mRNA and protein gene expression indicates that to form endothelial cells, hiPSCs developmentally differentiate first into a posterior primitive streak-like stage (indicated by high T and low FOXA2 expression), then into a heterogeneous population of mesodermal subsets (day 4). Subsequently, lateral plate mesoderm cells predominate over intermediate or paraxial mesoderm. To understand the role of BMP4 in this process, each

factor was withheld from various stages of the protocol. Results indicate that before day 4, BMP4 alone is necessary and sufficient to direct cells through posterior primitive streak into mesodermal progenitors that upon subsequent VEGF/FGF2 exposure can give rise to $CD31^{+}CD144^{+}KDR^{+}$ endothelial-like cells. In contrast, BMP4 is dispensable after day4, whereas VEGF and FGF2 are dispensable in the first 4 days of the protocol. To develop a disease model hiPSCs from patients with BMPR2 mutations associated with pulmonary hypertension were generated by reprogramming their archived fibroblasts. By differentiating these patient-specific iPSCs into mesodermal progenitors and ECs using our protocol, preliminary results indicate that the induction of mesodermal cells by day 4 was diminished in cells carrying BMPR2 mutations,, but whether their efficiency of differentiation into ECs is affected by these mutations remains in question. It can be concluded from this project, that we develop an in vitro differentiation model that replicates the developmental pathways of mesodermal and EC derivation in embryos, and suggests that BMP4 is necessary and sufficient to derive mesodermal subsets with EC competence but is dispensable for subsequent endothelial lineage specification.

TABLE OF CONTENTS

LIST OF TABLES

LIST OF FIGURES

LIST OF SCHEMES

LIST OF ABBREVIATIONS

Ac-LDL	Acetylated low density lipoprotein
ALK	Activin-like receptor kinase
BMP4	Bone morphogenetic protein 4
BMPR	BMP receptor
CB-ECFC	Cord blood ECFC
CReM	Center for Regenerative Medicine
CXCR4	C-X-C chemokine receptor type 4
Dkk1	Dickkopf homolog1
DMEM	Dulbecco's Modified Eagle Medium
DMSO	Dimethyl Sulfoxide
DNA	Deoxyribonucleic acid
EC(s)	Endothelial cell(s)
ECFC	Endothelial colony forming cells
EGM-2	Endothelial cells growth medium – 2
EMT	epithelial to mesenchymal transition
eNOS	Endothelial nitric oxide synthase
EP	Endothelial progenitors
ER	Endoplasmic reticulum
Evx1	Even-Skipped Homebox 1
FACS	Fluorescence-activated cell sorting
FBS	fetal bovine serum
FGF2	Fibroblast growth factor 2
FGFR	FGF receptor
FOXA2	Forkhead box A2

FOXC1	Forkhead box C1
FOXC2	Forkhead box C2
FOXF1	Forkhead box F1
GDF	growth and differentiation factor
GFP	Green fluorescence protein
hEGF	human epidermal growth factor
hESC(s)	Human embryonic stem cells
HGF	hepatocyte growth factor
hiPSC(s)	Human induced pluripotent stem cell(s)
HoxB1	Homebox B1
HPAH	Heritable PAH
HUVEC	Human umbilical vein endothelial cells
ICAM-1	Intercellular Adhesion Molecule 1
ICM	Inner cells mass
IGF-1	Insulin-like growth factor
IL-6	Interleukin – 6
IMR-90	Human foetal lung fibroblasts
KDR	Kinase Insert domain receptor
KLF4	Kruppel Like Factor 4
LIF	Lymphocyte inhibitory factor
MACS	Magnetic activated cell sorting
MEF(s)	Mouse embryonic fibroblast(s)
mRNA	Messenger RNA
NRP-1	Neuropilin-1
Oct4	Octamer-binding transcription factor 4

PAEC(s)	Pulmonary artery endothelial cell(s)
PAH	Pulmonary arterial hypertension
PASMC(s)	Pulmonary artery smooth muscle cell(s)
Pax2	Paired Bonx 2
PBS	Phosphate-buffered saline
PCR	Polymerase chain reaction
PLGF	Placental growth factor
PS	Primitive streak
RT-qPCR	Quantitiative RT-PCR
RNA	Ribonucleic acid
rRNA	ribosomal RNA
RT-PCR	Reverse transcription PCR
RUNX1	Runt-related transcription factor 1
SCID	Severe combined immunodeficiency
Sox2	Sex determining region Y Box 2
SSEA-1	Stage-specific embryonic antigen 1
STEMCCA	Single lentiviral stem cell cassette
TBX6	T-Box 6
TGF-β	Transforming growth factor beta
TRA	Transcription associated protein
VEGF	Vascular endothelial growth factor
vWF	Von Willebrand factor

CHAPTER I. INTRODUCTION

1.1 Significance

Endothelial cells are highly differentiated cells that are involved in several physiological processes such as angiogenesis, vasculogenesis, inflammation, coagulation and anticoagulation, vascular permeability, vascular tone and blood pressure. They are part of almost every human organ, therefore generating blood vessels and its basic unit, ECs, is a crucial and key step in any effort to regenerate any organ. Disturbance in the function of ECs have been linked to several human fatal diseases such as pulmonary arterial hypertension (PAH). Therefore our goal in this project was to develop an in vitro model to derive endothelial cells that we can use for future regenerative or disease models.

We chose to derive these endothelial cells from human induced pluripotent stem cells (iPSCs). By being induced from human adult somatic cells, hiPSCs cells do not only overcome the ethical concerns associated with the isolation of human embryonic stem cells (ESCs), but they also offer an unlimited source from any patient of pluripotent stem cells that can differentiate to all cell derivatives of the three embryonic germ layers (mesoderm, endoderm and ectoderm). As hiPSCs are patient specific, they offer the possibility of being used as 1) autologous graft, overcoming the hurdle of allogeneic rejection 2) disease models, or 3) models for drug discovery. Also as hiPSCs resemble human late epiblast cells of post-implantation embryos, these cells offer an in vitro model to study development and generate cells of different lineages using directed differentiation protocols as proven by several studies.

To derive ECs from hiPSCs, we chose a directed differentiation approach aiming to replicate those steps that are involved in the derivation of ECs during embryogenesis and

development. By adopting this approach we are hoping not only to increase the efficiency of EC derivation but also to study factors that are involved in induction and specification of their progenitors. In addition, using a developmental approach to derive ECs, ensures that their phenotype is freshly patterned without the confounding effects of disease or environmental exposures that is thought to alter the epigomes and phenotypes of ECs throughout life. The de novo derivation of ECs from iPSCs ensures epigenetic marks and EC phenotypes are specified anew through the simulation of embryonic development in vitro. Hence, in case we want to develop organ or site specific ECs, it is important to derive them in a developmental approach in order to preserve those initial epigenetic patterns.

To develop this in vitro differentiation model, we will first review the embryonic development of ECs, the involved factors and signaling pathways, hiPSCs and previous efforts of deriving ECs from hiPSCs. We will also review the disorder, heritable pulmonary arterial hypertension (HPAH), since iPSC-derived ECs can be used as tool to possibly understand the pathogenesis of this disease.

1.2 Embryonic development of mesoderm and endothelial cells

To differentiate hiPSCs into ECs, it is important to review the embryonic stages and factors that are involved in the derivation of ECs.

1.2.1 Early embryonic development and gastrulation

Fertilization of oocytes marks the beginning of embryo development, where the zygote is formed and will undergo a series of mitotic divisions to give rise to a mass of 16 cells called the morula. After a series of further cell divisions and as the morula enters the uterine cavity, a fluid-filled cavity forms called the blastocele, and at this stage the

embryo is called a blastocyst. The outer layer of the blastocyst, trophectoderm, gives rise to portions of the yolk sac and placenta. The inner cells of the blastocyst are called the inner cell mass (ICM) and will form the entire fetus as well as the extra-embryonic mesoderm. The ICM undergoes rapid proliferation and differentiation to form the epiblast. A transient structure called the primitive streak (PS) will be formed in the posterior epiblast and its formation will mark the onset of a process called gastrulation in which the three embryonic germ layers will be established. With time, the PS extends anteriorly (disto-anterior) and will end at approximately mid epiblast in location called the primitive node (1,2).

During gastrulation, epiblast cells undergo an epithelial to mesenchymal transition (EMT), lose E-cadherin, mobilize and move through the PS and exit either as mesoderm or definitive endoderm (2). Based on several molecular and lineage tracing and mapping studies, the anterior-posterior regions of the PS were found to have different gene expression patterns and developmental potential. Posterior primitive streak cells express HoxB1 and Evx1 and the epiblast cells that traverse through it will give rise to extra-embryonic and lateral plate mesoderm. Cells that migrate through the more anterior region of posterior PS will give rise to intermediate mesoderm and paraxial mesoderm. Anterior PS expresses Foxa2 and the epiblast cells that traverse through it will give rise to definitive endoderm. This anterior-posterior patterning of the PS strongly suggests that it is tightly controlled by different signals and factors secreted from cells in the different regions of PS or in close proximity to it (1-4).

Among several signaling pathways that are involved in gastrulation and PS formation, members of the TGFb family (BMP and Nodal), Wnt family and their antagonists were found to be essential in this anterior-posterior patterning of PS and its subsequent lineage specification. Nodal and Wnt3 are expressed at the posterior epiblast and found to induce

PS formation starting from that location (5-7). Whereas Wnt inhibitor; DKK1 and Nodal inhibitor; Cerberus-like and Lefty1 were found to be expressed in anterior visceral endoderm (anterior epiblast) (8-11). This regional expression of Nodal, Wnt3, and their antagonist establishes a gradient of Nodal and Wnt3 expression along the anterior-posterior axis of the embryo and is found to be essential for anterior patterning of epiblast and to restrict PS formation to the posterior epiblast. At late PS stage, Nodal expression become restricted to the primitive node, the most disto-anterior region of PS with very low concentrations at the posterior region of embryo. BMP4 is secreted from extra-embryonic ectoderm adjacent to the proximal end of the epiblast, while its inhibitors; Chordin and Noggin is expressed at the distal end of the epiblast (12-15). Such pattern of Nodal and BMP expression established a reversed Nodal and BMP4 gradient along the disto-proximal axis of the embryo. The results of several studies indicate that this reversed Nodal and BMP4 gradient is important in inducing mesodermal lineages and endoderm along the anterior-posterior axis of PS and suggest that high level of BMP4 and Nodal are required for inducing mesoderm and endoderm respectively (1-4).

1.2.2 Mesoderm development, specification and derivation of endothelial cells.

As mentioned previously, cells that traverse through PS will exit either as mesoderm or endoderm. Mesoderm cells are specified along the mediolateral axis into paraxial, intermediate and lateral plate mesoderm. This specification was found to be dependent on the concentration of BMP4, in which lateral plate mesoderm expresses higher levels of BMP4 than paraxial mesoderm and at the same time, paraxial mesoderm was found to express the BMP4 antagonist Noggin (16,17). It has been suggested that BMP4 is specifying the mesodermal layer by inducing differential expression of Forkhead (FOX) family of transcription factor, in which FOXF1 is expressed in lateral plate mesoderm, while FOXC1 and FOXC2 are expressed in paraxial mesoderm (18,19).

Paraxial mesoderm will produce somites on either side of the neural tube, which in turn produce muscular and skeletal elements of vertebrate. The anterior-most paraxial mesoderm along with neural crest will form the connective tissue, muscular and skeletal elements of face and skull. The intermediate mesoderm will generate the kidneys, gonads and the cortical portions of the adrenal gland (1).

Lateral plate mesoderm will split horizontally into two layers, the dorsal (somatic or parietal) and ventral (splanchnic or visceral) layers. The splanchnic layer together with the endoderm will form the wall of gut tube and the cardiovascular lineages, while somatic layer along with ectoderm will form folds that will generate dermis of the skin, skeletal and muscular elements of the limbs. It will also form the extra embryonic mesoderm (1).

The development of endothelial cells and blood vessels starts with the commitment of progenitor cells and their migration from posterior primitive streak into the extra-embryonic yolk sac and into the embryo proper to form the extra embryonic and intra-embryonic vascular network. The receptor tyrosine kinase Flk-1 is considered to be one of the markers for these progenitor cells based on findings of several studies. Dumont et al found that Flk1 at the primitive streak stage is expressed in the extra embryonic, paraxial and lateral plate mesoderm (20). Ema et al confirmed Flk1 expression using Flk1-lacZ knock-in model (21). Shalaby et al found that mice deficient in Flk1 display defect in blood island, blood vessels and endocardium and die around E9.5 (22). Lee et al demonstrated that in Er71 (member of Ets transcription factors and inducer of Flk1+ mesoderm) deficient mice were able to gastrulate, but lacked the expression of Flk1 and died around E9.5 due their inability to develop blood, vessels, and endocardium, similar to Shalaby et al findings (23). Differentiation and Fate mapping studies demonstrated that Flk1+ mesoderm cells contributed to hematopoietic, endothelial, skeletal and smooth

muscle cells (24-28). Huber et al used transgenic mice with green fluorescence protein (GFP) targeted to brachyury locus and showed that Flk1+ cells, before migrating to the yolk sac, co-express Brachyury (T) and present in highest frequency in the posterior primitive streak. When they isolated streak cells and cultured them in vitro, they found that endothelial cells were derived only from the $T^{+}Flk1^{+}$ cells, confirming the finding of previous studies, that $Flk1^{+}$ is a reliable early marker for mesodermal progenitors of endothelial cells (29). VEGF is one of the ligands of Flk1, and is found to be expressed in endoderm juxtaposed to Flk-1 expressing mesoderm at E7.0. This complementary expression profile of VEGF and Flk-1 continues throughout development and can be seen later on in organs that are being vascularized by the angiogenesis process (20,30,31). Carmeliet et al used a VEGF deficient mouse model and found that these mice died due to abnormal blood vessel formation, similar to previous reports using a Flk-1 deficient mouse model (32). These findings indicate the importance of VEGF/Flk1 in mesoderm specification and that it is indispensable for the derivation of endothelial cells and vascular system development. Another important signaling pathway for mesoderm specification and derivation of endothelial cells is FGF signaling. It has been challenging to study the role of FGF signaling in the derivation of endothelial cells and vascularization as disturbing the gene encoding FGFR1/2 results in embryonic death before gastrulation (33,34). Lee et al were able to solve this challenge with the use of adenovirus-mediated expression of dominant-negative FGFR-1 in mouse embryos. They found that FGFR-1 is required for the development and maintenance of the vasculature in the embryo (35).

To have a better understanding of the further specification of mesodermal progenitor cells into endothelial cells, it is important to address the much debated question of whether hematopoietic and endothelial cells share the same bipotent mesodermal progenitor,

referred to as the hemangioblast. Sabin et al first observed undifferentiated mesoderm cells migrated into the area vasculosa of the chick yolk sac and then differentiated into highly proliferative cells that form a solid cell mass. The outer cellular layer of this mass differentiated into endothelial cells while the blood plasma appeared to derive via liquefaction of the central core during vessel lumen formation. Furthermore, primitive erythroblasts appeared to directly bud from vascular endothelial cells. The differentiation of these two cell types, endothelium and erythrocytes, from similar undifferentiated mesodermal cells and the budding of primitive erythroblasts from endothelial cells lead to the assumption that endothelial and hematopoietic cells arise from the same progenitor cell, and Sabin et al initially called this cell an “angioblast" (36). In the 1930s, Murray re-branded Sabin's "angioblast" as a "hemangioblast," to emphasize the two cell types deriving from this putative common progenitor (37). Circumstantial evidence provided in support of this common progenitor is the observation that the progenitors for endothelial and hematopoietic cells share common markers such as Flk1, Scl, lmo2, Tie1, Tie2, CD31, CD34 (22,38-42). Huber et al were able to isolate progenitor cells that co-express brachyury and Flk1 from primitive streak, and these cells were able to give rise to cells of hematopeitic, endothelial and smooth muscle lineages after in vitro culture (29). Supporting Huber et al’s findings, Vogeli et al in single cell fate mapping study using zebrafish embryos, showed that at least a proportion of the cells appeared to give rise to both hematopoietic and endothelial cells (43). However, arguments against the existence of a bona fide hemagioblast came from several studies which showed that endothelial and hematopoietic lineages do not appear to arise from a primitive streak-derived bipotential common precursor, but rather are derived from independent epiblast populations (44-46). Also, regarding the point that the progenitor of both lineages share similar makers can be challenged by the fact that knockout or knockdown experiments to study markers that can

delineate these lineages are not possible yet as all tested markers so far caused disturbance both in blood and vascular system, so they showed that these markers are important for both lineages, but did not for fact show that there single progenitor for both lineages actually express these markers (45). Another challenge to the findings of Huber et al (29), is criticism that the work is based solely on in vitro cultures as these investigators did not test the fate of these progenitors in vivo and did not provide lineage tracing developmental models. Hence, Huber et al had defined $Bry^{+}Flk1^{+}$ cells as hemangioblasts, based on in vitro potential but not fate. More recent studies now suggest that a common progenitor for the earliest definitive hematopoietic cells may be endothelial cells in specific vascular beds within the developing embryo, now referred to as "hemogenic endothelium". These cells were first observed in experiments where blood cells were found to be generated from a subset of phenotypically differentiated endothelial cells on the wall of the embryonic aorta in a region referred to as the aorta-gonad-mesonephros (AGM.) (42,47). The concept of hemogenic endothelium was supported by Sugiyama et al, who used Ac-LDL-DiI to label endothelial cells at E10, and found that Dil positive erythrocytes were generated, indicating that they were potentially endothelial cell-derived (48). A middle ground to the hemangioblast vs. hemogenic endothelium debate was proposed by Lancrin et al, wherein the mesodermally-derived hemangioblast gives rise to an endothelial intermediate (hemogenic endothelium) that then gives rise to hematopoietic cells (49). They found that the transcription factor Scl is indispensable for the establishment of hemogenic endothelium, while the core binding factor Runx1 is critical for the generation of a definitive hematopoietic cell. The role of Runx1 is further supported by Chen et al (50).

From previous sections, we reviewed the developmental stages that are involved in the derivation of endothelial cells, starting from the formation of PS, to lateral plate

mesoderm and specification to endothelial progenitor cells. We also reviewed the important factors that are involved as well such as members of TGFb (BMP and Nodal), WNT family, VEGF and FGF. In the coming sections we will discuss the embryonic and induced pluripotent stem cells, and their differentiation into endothelial cells lineages.

1.3 Embryonic stem cells, induced pluripotent stem cells and differentiation

1.3.1 Embryonic stem cells

In 1981 Evans and Kaufman et al was the first to report the isolation and culture of pluripotent stem cells from mouse embryos at the blastocyst stage. The isolated cells had normal karyotype, expanded and maintained in an undifferentiated state, made embryoid bodies in vitro and formed teratomas in vivo. They termed these cells as EK (51). In the same year Gail R. Martin described a different method of stem cell isolation and culture, in which they used medium conditioned by teratocarcinoma stem cells to maintain the isolated pluripotent stem cells. Beside the characteristics that were described by Evans et al, the isolated pluripotent stem cells expressed the pluripotent marker SSEA-1. Martin et al was the first to refer to these cells as embryonic stem cells (EC cells) (52).

Thomson et al isolated the first human ES cells (hESCs) from an in vitro fertilized egg in 1998. The isolated cells had normal karyotype, express high levels of telomerase (indication of high replicative potential), express pluripotent markers (SSEA-3, SSEA-4, TRA-1-60, TRA-1-81 and alkaline phosphatase) and formed teratomas after injection into SCID mice. These teratomas contained derivatives of all three germ layers and in vitro the isolated ES cells differentiated into endoderm and trophoblast (53).

The ability of ES cells 1) to indefinitely symmetrically self-renew while maintaining normal karyotype and 2) to differentiate in vivo and in vitro to cells of all three germ

layers, made them a valuable tool to study developmental biology, for drug discovery and to be a potentially unlimited source of functional human cells for regeneration and tissue engineering. The main obstacles preventing research progress in their clinical application have been the ethical controversy related to their isolation from human embryos and the possibility of allogeneic rejection of cells derived from ES cells if they were to be transplanted into patients.

1.3.2 Induced pluripotent stem cells and reprogramming

Shinya Yamanaka hypothesized that factors which maintain the identity of ES cells, are also able to induce pluripotency of somatic cells. His hypothesis emerged from three scientific discoveries in stem cells, developmental biology and genetic engineering fields. The first is somatic cell nuclear transfer to accomplish reprogramming by transferring the nucleus of adult differentiated cells into enucleated oocytes or by fusing differentiated cells with ES cells (54,55). Both methods revealed that the nucleus of even differentiated cells contains all the genetic information required for the development of entire organism and that the oocytes or ES cells contain factors that are able to reprogram somatic cell nuclei. Second is the discovery of master transcription factors that can induce the fate of different lineages (56,57). Third is the isolation of ES from mouse and human blastocytes (51-53). Yamanaka and his student Kazutishu Takahashi were able to induce pluripotent stem cells from mouse embryonic and adult fibroblasts by retroviral transduction of four transcription factors (Oct3/4, Soc2, c-Myc, and Klf4) under ES cell culture conditions. They called the isolated cells; induced pluripotent stem cells (iPSCs). The isolated iPSCs express pluripotent markers and had similar morphological and growth properties to ES cells. In addition, iPSCs formed teratomas that contain tissues from all three germ layers upon their transplantation in nude mice. Finally when iPSCs were injected into mice blastocysts, they contributed to mouse embryonic development (58). One year later the

same group along with Thomson et al were able to generate iPSCs from human somatic cells (59,60). The generation of iPSCs not only represents a solution to the ethical controversies and allogeneic rejection hurdles associated with ES cells but can also open the door for disease modeling and genetic correction of patient specific lines.

The ability to induce pluripotent stem cells from human somatic cells is considered a paradigm shift in the field of stem cells, developmental biology, genetic engineering and tissue regeneration. In addition, since these cells resemble human late epiblast cells of post-implantation embryos, these cells offer an in vitro model to study development and generate cells of different lineages using directed differentiation protocols as proven by several studies (3,4).

Despite the great potential of iPSCs, there are several issues that still need to be resolved to allow them to reach their full potential. First, unlike mouse iPSCs that are considered to be naive cells, hiPSCs, are seen as primed cells that might be biased toward specific differentiation potential. Second, the reprogramming process might result in incomplete or partially reprogrammed iPSCs, which can affect the pluripotency of the cells and result in defective differentiation. Third, are the challenges related to the reprogramming technique itself. The original re-programming technique used retroviral transduction of Oct3/4, Soc2, c-Myc, and Klf4 to induce pluripotency, such a technique has low iPSCs derivation efficiency (0.02%) and the integration of the viral vector in the host genome poses several risks, such as disturbing or activating neighboring genes. In addition, any potential reactivation of the reprogramming factors especially cMyc might be oncogenic (61,62). These challenges potentially limit the use of iPSCs in clinical and transplantation therapies. To overcome these challenges, several studies have offered techniques to increase reprogramming efficiency and to minimize or avoid integration into the host genome.

Sommer et al, designed a single lentiviral stem cell cassette vector (STEMCCA) encoding the reprogramming factors (Oct4, Sox2, Klf4 with or without c-Myc) and flanked by loxP sites. With the use of STEMCCA the authors reported derivation of iPSCs with 0.5% efficiency (63). A humanized version of STEMCCA was constructed later with similar efficiency (64). With such design, STEMCCA addressed two issues, first avoiding the use of multiple single viral vectors to deliver the reprogramming factors, resulting in higher efficiency than what previously reported. Second the ability to produce transgene free iPSCs, by using a Cre/loxP system to excise STEMCCA makes the generated iPSCs more suitable for clinical therapies and transplantation (63-65).

Other integration free methods for reprogramming have been introduced. Adenovirus is considered to be an option, as it is a non-integrating virus, however the reported efficiency was very low (0.0001-0.001% and 0.0002% in mouse human cells respectively) in comparison to other methods (66,67). Sendai virus has been successfully used to reprogram blood and neonatal and adult fibroblast cells with an efficiency of 0.1-1% in approximately 25 days. Beside the relatively high efficiency, Sendai virus is an RNA based virus which replicates in the form of negative-sense single stranded RNA in the cytoplasm of infected cells and does not go through a DNA phase nor integrate into the hose genome. It dilutes out of cells approximately 10 passages after infection which is considered an advantage and disadvantage at the same time (68,69). Warren et al were able to generate iPSCs from human fibroblast with an efficiency of 1.4% using mRNA transfection and this efficiency increases to 4.4% when they added Lin28 to the 4 reprogramming factors and valporic acid in the cell culture medium (70). Other reprogramming methods were used as well such as PiggyBac vector (71), Minicircle vectors (72) and Episomal plasmids (73).

1.4 Derivation of Endothelial Cells (ECs) from hiPSCs

ECs are highly differentiated cells that perform multiple important functions such as angiogenesis, vasculigenesis, and the regulation of inflammation, coagulation and anticoagulation, vascular permeability, vascular tone and blood pressure. Many laboratories are developing protocols to derive ECs from hiPSCs. In the coming sections we will quickly review the assays and markers that are used to identify endothelial cells, then will review several differentiation protocols of hESCs and hiPSCs into endothelial cells.

1.4.1 Endothelial cells characterization assays and markers

There is no single distinct marker of ECs, instead a combination of markers are used for EC identification. The most commonly tested endothelial markers are PECAM (CD31), vascular endothelial (VE)-cadherin (CD144), endothelial nitric oxide synthase (eNOS), von Willebrand Factor (vWF), vascular endothelial growth factor receptor-2 (VEGFR-2, FLK1, KDR), and Tie-2. A number of functional assays were used to characterize the phenotypes of ECs, such as the release of nitric oxide by ECs that can be measured in vitro (74). The uptake of acetylated low-density lipoprotein is another characteristic of healthy ECs (75). Another assay is monitoring the upregulation of adhesion molecules including ICAM-1 in respond to inflammatory cytokines, such as TNF-alpha (76). In vitro angiogenic and vasculogenic assays that require EC proliferation and migration are conducted by seeding ECs onto growth-factor reduced Matrigel and observing tube-like networks that contain lumens. Such assays were also conducted in vivo by suspending cells into a Matrigel plug which was then subcutaneously injected into an immune-deficient animal. The Matrigel plug can later be removed and functional blood vessels can

be identified by the expression of endothelial species-specific markers in cells lining new blood vessels and presence of blood cells within the formed vessels (77,78).

1.4.2 Derivation of endothelial cells from hiPSCs

Over the last decade there was significant progress in the differentiation of hPSCs to ECs, with many studies using different differentiation protocols. These protocols can be grouped into 1) protocols using three dimensional embryoid bodies in a suspension culture, 2) differentiation by co-culturing hiPSCs with type of stromal cell to promote endothelial cell differentiation and 3) differentiating hiPSCs in monolayer (two dimension culture) on culture plates coated with protein substrates (Matrigel, gelatin or fibronectin). EB based differentiation protocols evolved from allowing spontaneously differentiating hESCs and hiPSCs EB to protocols that used FBS as the main differentiation factor to protocols that are serum free and depend on exogenous factors added with specific concentrations and exposure times. Levenberg et al. differentiated hESC-derived EBs, by withdrawing lymphocyte inhibitory factor (LIF) and bFGF and by day 13 they showed that 2% of cells expressed CD31. Upon isolation using flow cytometry, the isolated cells express other endothelial markers (CD144 and vWF) and were able to form tube like structure in vivo containing mouse blood cells (79). Yu et al, went one step further, they used two steps protocol, in which they differentiated hESC-EBs by using a 20% fetal bovine serum (FBS) based media for 4 days. Then the differentiated EBs were cultured for an additional 8 days in endothelial cell growth medium-2 (EGM-2) which contains 2% FBS, 0.04% hydrocortisone, 0.1% heparin, 0.1% human epidermal growth factor (hEGF), 0.1% long R3-human insulin-like growth factor (IGF-1), 0.1% ascorbic acid, 0.4% human fibroblast growth factor (hFGF)-B, 0.1% vascular endothelial growth factor (VEGF), 0.05% gentamicin, and 0.05% amphotericin-B. They reported that their differentiation protocol consistently yielded >10% cells that express CD31 and upon

isolation, more than 90% of the isolated population expressed CD31 and CD144 (80). Rufaihah et al used a similar approach, but they added BMP4 and VEGF in a 20% FBS containing media for the first 4 days, and then they withdraw BMP4 for next 10 days. They reported 5-20% of cells expressing CD31 by the end of the protocol. They also reported that the isolated CD31 cells co-express CD144 and vWF and were able to promote the formation of capillary like structure in vivo that contain mouse blood cells, although it was unclear whether the injected cells actually integrated as ECs in the new vessels vs provided paracrine secreted factors to promote the growth/survival of endogenous mouse ECs (77). James et al. used a serum free differentiation media that contains BMP4, Activin and FGF2 and VEGF. These conditions generated relatively sparse population of ECs as indicated by a VE-Cadherin-GFP reporter (0.2%). However, inhibition of TGFβ at day 7 increased endothelial differentiation efficiency by 10-fold. Subsequent TGFβ inhibition of magnetic activated cell sorting (MACS)-purified CD31+ cells increased their expansion 36-fold (81). White et al, used hESCs and hiPSCs to derive endothelial cells. First they generated KDR+ cells using a media that contained BMP4, Activin A and bFGF and by day 4 they reported that 55% of the cells express KDR. At day 4 they plated EB on fibronectin coated plate and differeniated them using bFGF and VEGF. By day 6 they sorted KDR^{high} and found that more than 90% of the cells express CD31 and CD144. The sorted cells express vWF, formed tube-like structure in vitro and functional blood vessels in vivo (82). These studies indicate that manipulation of specific signaling pathways following the initial differentiation to EC progenitors increases cell proliferation and conservation of the EC phenotype, approaches which could prove vital in the derivation of tissue-specific ECs. Pure populations of ECs can be readily obtained using EB differentiation protocols because of the ease of sorting and expanding cells expressing EC markers.

Co-culturing of pluripotent stem cell with stromal cells is another way to derive endothelial cells. Vodyanik et al, cultured hESCs on OP9 for 9 days using an alpha-MEM based medium that contains 10% FBS. By day 9, they sorted CD34+CD43-KDR+ cells and plated them on gelatin with endothelial maintenance media. The plated cells, expressed CD31, CD144, and formed tube like structures in in vitro Matrigel assays (83). Choi et al used the same strategy, but they sorted CD34+CD43-CD31+ cells at the end of the differentiation protocol (84).

Monolayer-based differentiation protocols using growth factors, and extracellular matrix have also been used to derive endothelial cells from pluripotent stem cells. Wang et al, developed a monolayer differentiation protocol, based on the hypothesis that EB will trigger spontaneous differentiation of cells intro different cell lineages decreasing the efficiency of specific lineages such as endothelial cells. They used a differentiation media that contain 20% KSR, 50ng/ml of bFGF, BMP5 and VEGF. After 10 days they isolated CD34+ cells and plated them in gelatin coated plates in EGM-2 media. The isolated cells expressed endothelial markers (CD31, CD144), and formed functional blood vessels in vivo (85). Tatsumi et al differentiated hESCs in the presence of a glycogen synthase kinase-3β inhibitor and VEGF and found that about 20% of the population expressed CD144 and CD31. Upon MACS purification, the sorted cells were positive for diI-acetylated low-density lipoprotein uptake and formed capillary-like structures in vitro (75). Sahara et al. screened more than 60 bioactive molecules at different time points and developed a multi-step differentiation protocol, in which they treated the hESC and hiPSCs in the first 4 days with BMP4 and CP21R7 (GSK-3B inhibitor) to induce KDR+ cells, then for additional 2-3 days they used combination of VEGF, γ-secretase inhibitor DAPT (NOTCH signaling inhibitor), placental growth factor (PLGF) and hepatocyte growth factor (HGF) to generate endothelial progenitors (EP) cells that express CD31,

CD144, KDR and CD34 and finally they used VEGF for additional 7 days to generate mature endothelial cells. They compared EB and monolayer based differentiation protocols and found monolayer to be efficient. With this multi-step approach, they reported generation of approximately 20 million endothelial cells (EC) from 1 million hiPSCs. When they transplanted the hiPSCs derived EP, EC and control (HUVEC), in SCID mice, they reported that EP formed significantly more functional blood vessels than EC and HUVEC and these vessels lasted more than 3 months in the host without tumor formation. The authors conclude that the hESC/hiPSC-derived EP are more readily produced and display superior vessel forming ability compared to more mature EC and may be an attractive cell population for revascularization strategies in human subjects (86). Prasain et al. developed a protocol that relies on the use of BMP4, FGF2, VEGF and Activin (first 24hr) and the use of Neuropilin-1 (NRP-1) to identify a subset of EC co-expressing CD31 and CD144 that display functional properties similar to umbilical cord blood endothelial colony forming cells (CB-ECFC) with high clonal proliferative potential and robust in vivo vessel-forming ability. The ESC-NRP-1+CD31+ ECFC and iPSC-NRP-1+CD31+ ECFC maintained a stable endothelial phenotype and function and did not undergo replicative senescence for 18 passages in vitro. Given the high rate of proliferation, the iPSC:EC ratio was identified as $1:1 \times 10^8$. These hiPSC derived ECFC engrafted and formed functional human vessels in immunodeficient mice for > 6 months. Furthermore, they rescued the avascular regions and blunted the neovascularization observed in vehicle treated mice that had undergone oxygen-induced retinopathy induction. The authors concluded that this unique population of iPSC-NRP-1^+CD31^+ ECFC can provide clinically relevant numbers of highly functional EC that may be a useful cell therapy to employ in patients that display vascular dysfunction (78).

1.5 Heritable pulmonary arterial hypertension and BMPR2 mutation

Pulmonary arterial hypertension (PAH) is a disease of the pulmonary vasculature that is pathologically characterized by progressive neointimal proliferation leading to vasoocclusive lesions (87). It is also characterized by muscularization at the alveolar duct and wall level. Such muscularization is characterized by increased smooth muscle cells (SMCs) proliferation, which is believed to be stimulated by dysfunctional ECs, that either release factors that stimulate SMC proliferation, such as FGF-2 (88), or fail to produce agents that normally suppress proliferation of SMCs in response to growth factors, such as apelin (89). PA ECs from patients with IPAH produce decreased amounts of nitric oxide (NO) which is a vasodilator and suppressor of SMC proliferation (90). Several studies found that muscularization of SMCs, is not only caused by increase in SMCs proliferation, but also by migration and differentiation (transformation) of resident stem cells (91), fibrocytes (92), pericyte or even PA-ECs into SMCs (93,94). Later in disease, dysregulated EC proliferation lead to the development of plexiform lesions. These lesions may reflect clonal expansion of apoptosis-resistant ECs, or they may be derived from circulating endothelial progenitor cells (EPCs) that accumulate at sites of endothelial denudation or injury and expand locally (95,96). Clinically it is characterized by progressive dyspnea, exercise intolerance, increasing pulmonary vascular resistance, and ultimately right ventricular failure and death (97). Under the current classification system, WHO Group 1 PAH is divided into heritable (HPAH), idiopathic (IPAH), and PAH associated (APAH) with a variety of other systemic diseases or drug/toxin exposures (98). No therapies tested to date have shown any significant ability to cure or reverse the disease and untreated PAH results in death from right heart failure in less than 3 years for most patients (99).

1.5.1 Heritable Pulpmonary Arterial hypertension

In 1954, Dresdale et al described the familial transmission of PAH in a kindred, thus providing the first known reports of familial PAH, the heritable form of PAH. After almost 30 years, two independent teams of investigators mapped the locus for the gene, named PPH1, for HPAH to chromosome 2q31-32 (100,101). Subsequently, both teams also demonstrated that germline mutations in the gene encoding bone morphogenetic protein receptor type-2 (BMPR2), a transforming growth factor-β (TGF-β) superfamily of receptors member, was the gene responsible for the majority of cases of the autosomal dominant familial disease now known as HPAH (102,103). Investigators at Vanderbilt university identified a family which originally had 6 deaths related to PAH, they called this family, "family14" (as there was 13 previous families with HPAH). This family has mutation in the ligand-binding domain of BMPR2 (Scheme 1). Vanderbilt investigators followed this family and by 2011 they diagnosed 36 members with HPAH (29 females and 7 males) and at least another 48 members who were unaffected but who were obligate carriers of the mutation (104). The inheritance pattern in HPAH is best described as autosomal dominant with reduced penetrance which varies from 20%-80% (105,106). This reduced penetrance indicates that the mutation is the not the sole factor for developing PAH, and strongly suggests the presence of modifying genetic or environmental factors, which could increase or decrease the risk of developing PAH.

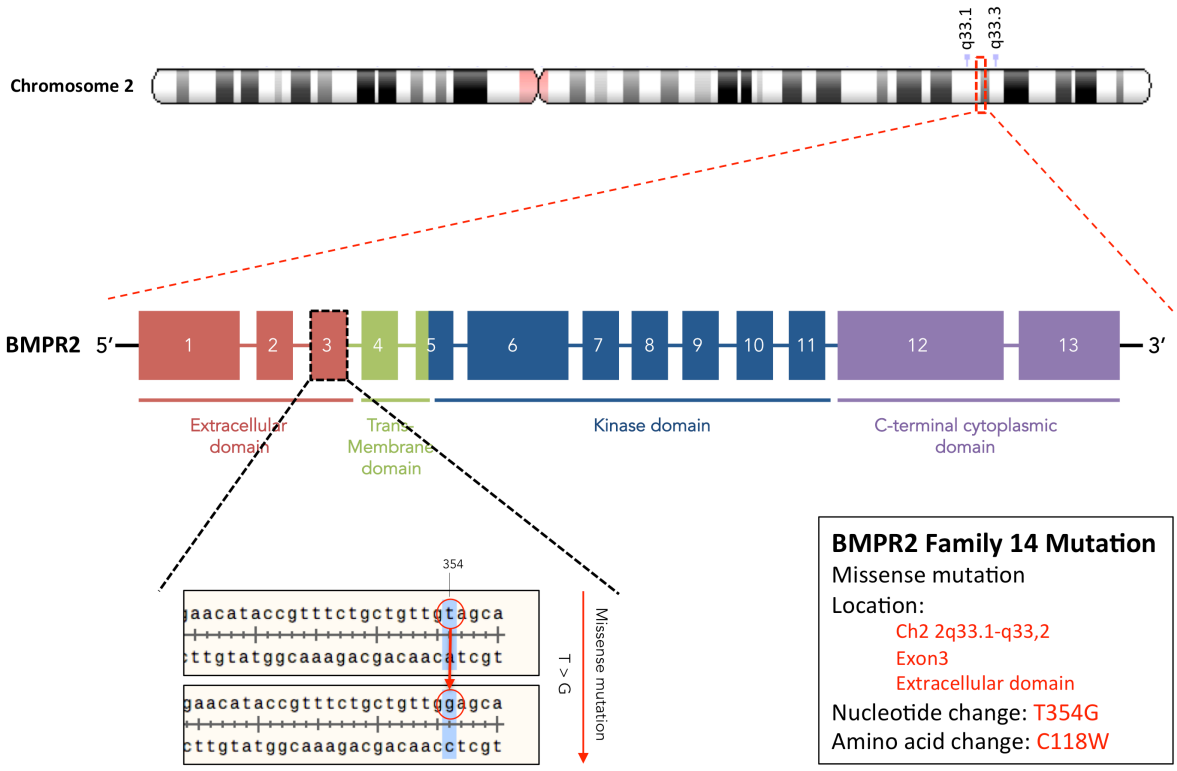

Scheme 1: Schematic on BMPR2 Family 14 Mutation

Top panel shows chromosome 2 with the location of BMPR2 gene. Middle panel shows BMPR2 gene which is composed of 13 exons and 4 domains. The lower panel with the box shows information on BMPR2 mutation

1.5.2 BMP signaling and BMPR2

BMPs are the largest group of cytokines within the TGF-β superfamily and were originally identified as molecules regulating growth and differentiation of bone and cartilage (107). BMPs are involved in regulating growth, differentiation, and apoptosis of several cell types, and are crucial signals in embryogenesis. They also contribute to the homeostasis and repair of adult tissues (107-109). TGF-β superfamily type II receptors are constitutively active serine- threonine kinases and form homodimers that exist constitutively or are recruited to receptor complexes upon ligand stimulation (110). The BMPR2 gene is comprised of 13 exons that encode for 4 major functional domains of the receptor; the extracellular ligand binding domain (exons 2-3), the transmembrane domain (exon 4), the serine/threonine kinase domain (exons 5-11), and a long cytoplasmic tail (exons 12-13) that is unique amongst the TGF-β receptor family members for its length (Scheme 1) (102,111). BMPR-II initiates intracellular signaling in response to specific ligands: BMP-2, BMP-4, BMP-6, BMP-7, growth and differentiation factor-5 (GDF-5), and GDF-6 (111). The majority of ligands (BMP-2, BMP-4, BMP-7, and GDF-5 and GDF-6) bind with high affinity to the type I receptors, predominantly BMPRIA activin-like receptor kinase-3 (ALK-3) or BMPRIB (ALK-6), and with very low affinity to BMPR-II. GDF-5 demonstrates specificity for BMPRIB (112). In contrast, BMP6 binds with high affinity to BMPR-II. After ligand binding, the type II receptor phosphorylates and activates a glycine-serine rich domain on the proximal intracellular portion of an associated type I receptor. In turn, the activated type I receptors phosphorylate cytoplasmic signaling proteins known as Smads (113). BMPs signal via Smads 1, 5, and 8, which must complex with the common partner Smad (co-Smad), Smad-4, to translocate to the nucleus and regulate the transcription of target genes (Scheme 2) (113).

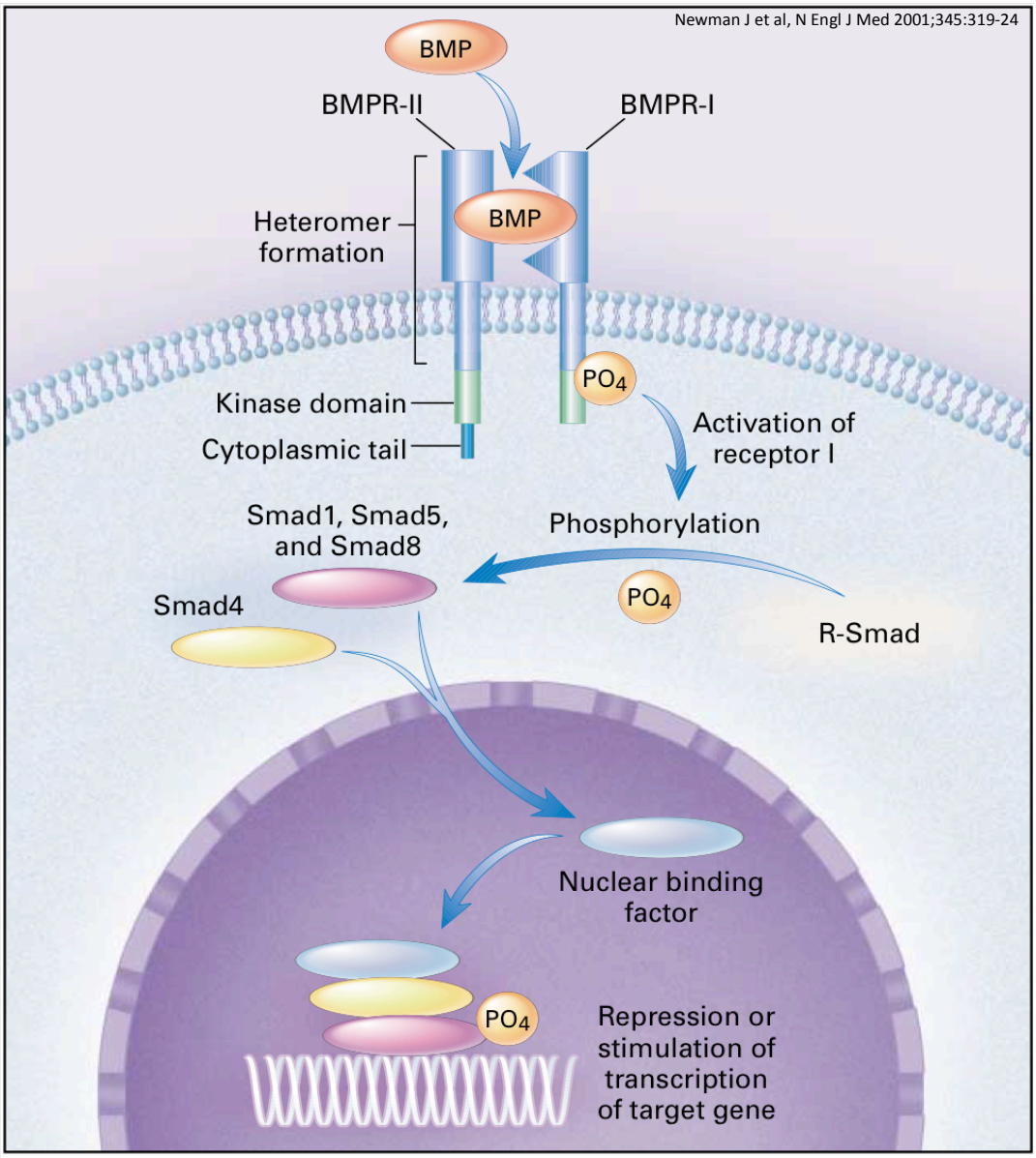

Scheme 2: Schematic representation of Bone Morphogenetic Proteins and Signaling

Bone morphogenetic protein receptors 1 and 2 (BMPR1 and BMPR2) are adjacent on cell membranes. Bone morphogenetic protein binds to the extracellular domain (ligand binding) of BMPR2, resulting in the formation of a heteromeric complex with BMPR1. BMPR2 then phosphorylates the transmembrane region of BMPR1, activating the kinase domain. The activated BMPR1 phosphorylates receptor Smad (R-Smad), thus activating one or more receptor-dependent cytoplasmic Smad proteins (Smad1, Smad5, and Smad8), which bind with Smad4 and migrate to the nucleus. The phosphorylated Smad complex attaches to a binding factor in the nucleus, and the resulting assembly either stimulates or represses gene transcription by interacting with DNA.

1.5.3 BMPR2 mutation and its impact on BMP signaling and HPAH

Several mutations were identified in BMPR2 coding regions including frame shift, missense, and nonsense mutations (102,103). While the majority of mutations affecting BMPR2 coding regions are frameshift, and nonsense mutation, about 30% are missense (114,115). These mutations are also affecting all BMPR2 domains, with increase risk of developing PAH related to mutations affecting kinase domain (116).

Morrell et al suggested that most of BMPR2 mutations disrupt BMP/Smad signaling by either affecting the trafficking of BMPR2 protein to the cells surface or the phosphorylation of type 1 receptor that in turn affects the downstream Smad signaling and transcription of target genes (117,118). Reduced trafficking of the mutant BMPR2 protein was found to be associated with missense mutations of cysteine residues within the ligand binding or kinase domain (118). Two explanations of such effect were suggested and both were linked to the retention of the mutant BMPR2 protein in the endoplasmic reticulum (ER). The first explanation state that the mutation leads to an unpaired sulfhydryl group, which could interact with other components of the ER chaperone, thereby preventing efficient trafficking of the protein. The second is that the unpaired cysteine causes interaction with the associated type I receptor, leading to failure of trafficking of both receptors. The later explanation was supported by Sobolewski et al, who reported that cysteine-substituted BMPR-II mutants retained within the ER prevented normal trafficking of BMPR1 receptor, but not wild-type BMPR-II (119). On the other hand, noncysteine mutations within the kinase domain reach the cell surface but fail to activate Smad-responsive luciferase reporter genes due to an inability to phosphorylate BMP type I receptors. Interestingly, BMPR-II mutants with missense mutations involving the cytoplasmic tail are able to traffic to the cell surface and are capable of activating Smad-responsive luciferase reporter genes to some extent but are

almost certainly relatively deficient in their ability to transduce signals via Smads (120,121).

Several mechanisms have been proposed to explain the effect of BMPR2 in developing PAH. Reduced BMP signaling due to BMPR2 mutation will cause imbalance between the TGFb and BMP signaling which is crucial for homeostasis and maintenance of lung vasculature. BMP4 was found to promote endothelial proliferation, migration and tubular formation (122). The opposite is true, in which knockdown of BMRP2 was found to increase the susceptibility of pulmonary artery endothelial cells (PAECs) to apoptosis (123). The response of pulmonary artery smooth muscle cells (PASMCs) is in contrast to PAECs, in which BMP signaling has inhibitory effects on PASMC proliferation, while TGFb promotes their proliferation (124). Such contrasting effects of BMP signaling on PAEC and PASMCs could explain the initial vascular damage and the later remodeling noticed in PAH. It has been suggested that BMPR2 mutations may compromise the integrity of pulmonary endothelial barriers by promoting endothelial cell apoptosis. In response to exposure of increased levels of TGFb (from ingress of serum factors through compromised endothelial barrier and those that are released from apoptotic endothelial cells (125)), and reduced level of BMP signaling due to BMPR2 mutation, PASMCs will proliferate at higher rates, which lead to muscularization of pulmonary vasculature, increasing vascular resistant and pulmonary hypertension. Also it has been proposed that increased apoptosis in the endothelium will favor the development of apoptosis-resistant clones of endothelial cells and lead to plexiform lesion formation (117).

Another mechanism by which BMPR2 mutations can contribute to PAH, is their effect on inflammation, as one key component in the pathogenesis of PAH is an increased level of inflammation manifested by elevated levels of inflammatory cytokines and infiltration of inflammatory cells. It has been found that the inhibition of inflammatory cytokines

(specifically NF-kB) is reduced in BMPR2 deficient cells, while increased TGF-B1 in the same cells, is related to the induction of interleukin (IL)-6 and IL-8 expression through inappropriately altered NF-kB signaling (126,127). Also loss of BMPR2 in the endothelial layer of the pulmonary vasculature could promote leukocyte extravasation into the pulmonary artery wall. This is supported by the findings that BMPR2 regulates the expression of CXCR2, which in turn regulates leukocyte migration and extravasation on endothelial cells (128). This was manifested in an in vitro study, in which Burton et al found that the enhanced transmigration of leukocytes observed in BMPR-II-deficient endothelium after tumor necrosis factor α or transforming growth factor β1 stimulation was CXCR2 dependent (129).

1.6 Hypothesis

After reviewing the embryonic development of ECs, the involved factors and signaling pathways, hiPSCs, previous efforts of deriving ECs from hiPSCs and HPAH, we formulated the following hypothesis:

1- Vascular endothelial cells can be generated in vitro from human pluripotent stem cells via the recapitulation of embryonic developmental milestones, beginning with the induction of primitive streak and mesoderm followed by specification into endothelium.

2- The resulting endothelial cells generated with this novel in vitro model can facilitate basic studies of human vascular development and can provide insights into the pathogenesis of vasculopathies such as heritable pulmonary arterial hypertension.

In the following chapter we will review the material and methods that we developed to test these hypotheses.

CHAPTER II. MATERIALS AND METHODS

2.1 Mouse embryonic fibroblast isolation, expansion and inactivation.

Mouse embryonic fibroblasts (MEFs) were obtained from our Center for Regenerative Medicine (CReM) stem cell bank. These cells were previously isolated from 13.5 day old mouse fetuses of timed-pregnant female mice that were purchased from Charles River Laboratories (BALB/c, strain code: 028). MEFs were thawed in MEF culture medium, consisted of Dulbecco's Modified Eagle Medium (DMEM) (Gibco)/10% heat-inactivated Fetal Bovine Serum (FBS) (Gibco)/1% Pen/Strep/1X L-glutamine (Gibco) and plated in $100cm^2$ culture dish. After expansion MEFs were inactivated via Mitomycin C (Fisher) treatment (10ug/ml for 2hrs) and were either frozen in 90% FBS/10% Dimethyl Sulfoxide (DMSO) (Sigma-Aldrich) freezing media or plated on gelatin-coated wells and used as feeder layers for iPSC culture.

2.2 Human skin fibroblast expansion and reprogramming

All human studies were approved by the institutional review board of Boston University and Vanderbilt University. Human dermal fibroblasts from patients with HPAH were obtained from Vanderbilt University. Four cells lines were received as detailed in table 1. To reprogram human dermal fibroblast, we used hSTEMCCA-loxP lentiviral vector, encoding the 4 human factors, OCT4, KLF4, SOX2 and cMYC that was previously described by Somers et al (64). A total of $1X10^5$ human fibroblasts were plated in DMEM with 10% FBS on a gelatin-coated 6-well plastic tissue culture plate. The next day polybrene was added to the media (5 ug/ml), and the cells were infected with hSTEMCCA-loxP lentiviruses at a multiplicity of infection (MOI) = 0.1, 1, or 10. On day 2, the media was changed to serum- free hiPSC media consisting of DMEM F12 (Gibco), 20% KnockOut Serum Replacement (Gibco), 1 mM nonanimal L -glutamine (Invitrogen),

0.1 mM b-mercaptoethanol (Invitrogen), 1% nonessential amino acid solution (Invitrogen), and 10 ng/ml of FGF2 (Invitrogen). On day 6 the entire well was trypsinized and passed at a 1:16 split by plating onto gelatin-coated 6 well tissue culture plate which had been preseeded the day before with mitomycin C-inactivated MEFs. hiPSC colonies were mechanically isolated 30-35 days postinfection based on morphology and expanded on MEF feeders in iPSC media. Candidate iPSC clones were screened by Southern blot to identify those carrying only one single integrated copy of hSTEMCCA, then they were characterized based on immunostaining with antibodies against stage-specific embryonic antigen 4 (SSEA-4), TRA1- 60, and TRA1-81 (ES Cell Characterization Kit, Millipore). Primary antibodies were detected with secondary Alexa Fluor 488 and 568 conjugated, goat anti-mouse IgG or IgM (Invitrogen).

To excise the hSTEMCCA vector, we used the method of Somers et al (64), in which hiPSC clones generated with hSTEMCCA-loxP lentivirus were transfected with a plasmid vector expressing Cre-recombinase and the Puro resistance gene. Briefly, hiPSCs were plated at different densities (1:20,1:40,1:60) in a 6-well plate (on MEFs) and cultured for 5 days with hiPSCs medium. Cells were transfected with Cre-excision transfection reagents; containing TransIT-HeLaMONSTER™ Transfection Kit (Mirus) and pHAGE2-EF1a-Cre-IRES-Puro-W plasmid. After 24 hours of transfection, cells were treated with hiPSCs containing 1ug/ml of Puromycin for 2 days, after that, the medium was changed to hiPSCs without Puromycin. After 13-15 days, surviving colonies were manually picked and replated into a 12-well plate and were expanded. gDNA of those colonies was extracted for PCR screening of hSTEMCCA excision.

Table 1: List of HPAH cell lines

	Vanderbilt ID	CReM Name	Phenotype	HPAH Status	Gender
1	Family 150	HAPH1	Mutation in BMPR2's exon 12 (2504delC)	Affected with HPAH	Female
2	Family 14	HPAH2	Mutation in BMPR2' exon 3 (354T>G)	Carrier	Male
3	Family 14	HPAH3	Mutation in BMPR2' exon 3 (354T>G)	Affected with HPAH	Male
4	Family 14	HPAH4	Mutation in BMPR2' exon 3 (354T>G)	Affected with HPAH	Female

2.3 Tissue culture of hiPSCs

HPAH iPSCs and normal control hiPSCs lines derived from individuals without any known vascular disease, specifically, BU1 (hiPSC clone BU1Cr-1), CF (hiPSC clone RC2 4-10-11) and 100-3 (hiPSC clone RC2 100-3), were all generated from dermal fibroblasts using the hSTEMCCA reprogramming system (64). These hiPSCs line were obtained from the CReM iPS cell bank (http://www.bu.edu/dbin/stemcells/index_iPSC.php). Undifferentiated hiPSCs were maintained and expanded on mitomycin C- inactivated MEFs, in hiPSC media. Cultures dishes and plates were coated with sterile gelatin (Millipore) before use. Cells were incubated at 37 C at 5% CO2. Approximately, every 5-7 days, cells were passaged using Collagenase IV (Invitrogen) and split into 1:6 ratio.

Undifferentiated hiPSCs were also adapted to feeder-free, serum-free conditions, in which, cells were maintained on Matrigel (Corning) coated 6-well plates in TeSR-E8 medium (StemCells technologies) in a 37 C incubator and 5% CO2. Approximately, every 5-7 days, cells were passaged using Gentle-Cell Disassociation Buffer (StemCells technologies) and split into 1:10 ratio.

2.4 Directed differentiation of hiPSCs into endothelial cells

On Day -2, sufficient volumes of TeSR-E8, DMEM/F12, and Gentle Cell Dissociation Reagent for passaging were pre-warmed. The well to be passed was washed with 1 mL of Ca2+/Mg2+-free phosphate-buffered saline (PBS). Wash buffer were aspirated and 1 mL of Gentle Cell Dissociation Reagent was added and the plate was incubated at 37°C for 8-10 min. Then cells were disloged by pipetting up and down 1-3 times using a pipette with a p1000 tip. Immediately the cells were transferred to a tube containing an equal volume of DMEM/F12. The well was washed again with 1 mL of DMEM/F12 to collect any remaining cells. The cells were centrifuged at 300 x g for 5 min. Then cells were re-suspended in 1 mL of single-cell passaging medium (TeSR-E8 supplemented with 10uM Y27632 Rock inhibitor (Sigma)) and numbers of live cells were counted using a hematocytometer. Cells were plated at desired density onto Matrigel-coated plates. (100,000 cells per 1 well of 6-well plate. This number was optimized for the BU1 hiPS cell line). Different cell lines needed different seeding densities. Cells were Incubated at 37°C and 5% CO2 for 48 hours.

On day 0, differentiation was induced by replacing TeSR-E8 media with BFV-A differentiation media (media consisting of: Stemline-II base media (Sigma), BMP-4, FGF2, $VEGF_{165}$ and Activin A (10ng/ml)(R&D)). At day 1 media was changed to BFV differentiation media (same as BFV-A, but without Activin A). Cells were fed every 2 days until day 12. On Day 4, cells were passaged and replated at a seeding density of 100,000 cells per 1 well of 6-well plate. By day10-12, cells were sorted as indicated in the text results, based on the expressing of endothelial markers; PECAM-1 (CD31), VE-cadherin (CD144) and VEGF receptor-2 (KDR). Staining for these markers was performed using the following antibodies: 1) Fluorescein Isothiocyanate (FITC) conjugated monoclonal mouse anti-human CD31 (BD bioscience, Cat no. 560984), 2)

Phycoerythrin (PE) monoclonal mouse anti-human CD309 (KDR) (BD bioscience Cat no. 560494 3) Alexa Fluor 647 monoclonal mouse anti-human CD144 (BD bioscience Cat no. 561567). Sorted cells were plated in matrigel-coated 12 well plates at a density of 2400 cells per well in EGM-2 media mixed 1:1 with EGM-2 containing BFV. Twelve days post sort, cells were passaged, replated (at a seeding density of $1x10^4$ cells/cm^2) and maintained in EGM-2 media.

2.5 Flow cytometry and fluorescence activated cell sorting (FACS)

Differentiating hiPSCs and endothelial cells were dissociated using TryplE 1X (ThermoFisher Scientific), washed with 2% PBS/2% FBS and stained for 30min on ice with monoclonal antibodies: Allophycocyanin (APC)-conjugated anti-human VE-cadherin (CD144), Phycoerythrin (PE)-conjugated anti-human VEGF receptor-2 (KDR), Fluorescein Isothiocyanate (FITC) anti-human PECAM-1 (CD31) (BD-Bioscience) and APC conjugated anti-human Neuropilin-1 (NRP-1)(Miltenyi Biotech). After cell staining, cells were washed with 1ml PBS/2% FBS, spun down at 300g/5min/4°C and cell pellets were either resuspended in PBS/2% FBS if analyzed or in PBS/2% FBS/1 X Pen/Strep if sorted. Cells were either analyzed using a FACSCalibur cytometer (BD Biosciences) or sorted using FACSAria III Cell Sorter (BD Biosciences). Data were analyzed using FlowJo software (Tree Star Inc).

2.6 Quantitative reverse transcriptase polymerase chain reaction (RT-qPCR)

Total Ribonucleic Acid (RNA) extraction was performed using miRNeasy Mini Kit (Qiagen) and 1ug DNAse-treated RNA was reverse transcribed using TaqMan Reverse Transcription Reagents (Applied Biosystems). qPCR of complementary deoxyribonucleic acid (cDNAs) was performed in a StepOnePlus real-time PCR system (Applied Biosystems) using TaqMan probes (table 2). Reactions were performed in triplicate.

Messenger RNA (mRNA) expression levels were normalized to 18S ribosomal RNA (rRNA) and quantification of relative gene expression presented as fold change compared to the relevant baseline was calculated using the 2-{delta}(delta}CT method. Biological triplicates from repeat experiments were used to calculate average fold change as well as the standard error of the mean (SEM) for each fold change in gene expression, represented by error bars where indicated.

Table 2: TaqMan inventoried primers

Cat #	Description
Hs00230962_m1	FOXF1
Hs01057416_m1	PAX2
Hs00365539_m1	TBX6
Hs00610080_m1	T
Hs00911700_m1	KDR
Hs01065282_m1	PECAM1 (CD31)
Hs00170966_m1	VE-Cadherin
Hs00204814_m1	FoxA2

2.7 Immunostaining

Cells were fixed with 4% (w/v) paraformaldehyde for 30 min and permeabilized with 0.1% (v/v) Triton X-100 in PBS for 5 min. After blocking with 10% (v/v) goat serum for 30 min, cells were incubated with primary following antibodies; anti-CD31 (R&D), anti-CD144 (R&D), anti-NRP-1 (Santa Cruz) overnight at 4 °C. Cells were washed with PBS, then incubated with secondary antibodies conjugated with Alexa-488 or Alexa-565 (Molecular Probe) and visualized by inverted and confocal microscopy after counterstaining with 2 g/ml DAPI (Sigma-Aldrich). The confocal images were obtained with an Olympus FV1000 mpE confocal microscope using as an Olympus uplanSApo 60xW/1.2NA/eus objective. All the images were taken as Z-stacks with individual 10-µm

thick sections at room temperature and images were analyzed using FV10-ASW 3.0 Viewer.

2.8 Acetylated low density lipoprotein (AC-LDL) uptake

Endothelial-like cells were incubated with 10 μg/mL DiI-Ac-LDL Alexa Fluor® 594 Conjugate (ThermoFisher) in complete EGM-2 media for 2 hours at 37°C. Then cells were examined for uptake of Dil-Ac-LDL using an inverted microscopy system at 10× magnification.

2.9 In vitro matrigel assay

Endothelial-like cells were disassociated and resuspended in EGM-2 media. Cells were plated at a density of 1.0×10^4 cells per well in triplicate in 96-well plates coated with 50μL of growth factor-reduced Matrigel (BD Biosciences). Plates were incubated overnight at 37°C. After 8-16 hours of incubation, photomicrographs were taken from each well at×10 magnification. Images were acquired using a SPOT RT color camera (Diagnostic Instruments) with the manufacturer's software. Phase contrast images were taken with air objectives. Images were analyzed using "Angiogenesis Analyzer" plug-in for ImageJ (Gilles Carpentier Research, http://image.bio.methods.free.fr/) to provide an automated quantitative assessment of network formation for the tested cell lines. The software quantified branches (elements delimited by a junction and one extremity), segments (elements delimited by two junctions), connecting segments (elements delimited by two junctions, none exclusively implicated with one branch) and meshes (area enclosed by segments or connecting segments) (130).

2.10 Correcting BMPR2 mutations using CRISPR/Cas 9 technology

Mutational analysis of the gene encoding BMPR2 in six affected members revealed that all have a T354G missense mutation in exon 3 that encodes an amino acid substitution of tryptophan for cysteine. Family 14 fibroblasts that we reprogrammed into hiPSCs, have T354G missense mutation in exon 3 of BMPR2 gene. This mutation resulted in amino acid substitution of tryptophan for cysteine. Correction was done using CRISPR/Cas9 technology, and Cas9 was delivered to iPSCs using plasmid transfection of pSpCas9(BB) (Addgene #62988) (131) engineered to over-express the Cas9 enzyme together with a gRNA targeting the BMPR2 3rd intron. Targeting plasmids were prepared as follows. First a guide RNA (gRNA) was designed using the Zhang lab design tool at http://crispr.mit.edu. The gRNA that was selected had the following sequence: 5'AAGGTTGAAGCCAGGCGTGA3', designed to bind to the intron region downstream to exon3 of BMPR2 locus. To clone the gRNA delivery plasmid, oligos encoding the gRNA were ordered from IDT. The donor vector was constructed to contain homology arms (HA) flanking the mutation site in the BMPR2 locus but containing the BMPR2 corrected sequence followed by a PGK promoter-driven floxed transgene encoding drug resistance selection cassette (Puromycin) and followed by polyA sequence. The left-HA was 830 bp long and 831 bp for the right-HA. The floxed antibiotic resistance cassette was designed to be in the intronic sequence adjacent to the mutant exon to be corrected.

Cloning of the Cas9 and gRNA delivery plasmid proceeded as follows: upon receipt of oligos, they were re-suspended to a final concentration of 100 uM. The top and bottom strand oligos were phosphorylated and annealed under the following conditions:

Amount (uL)	Component
1	gRNA top strand, 100 uM
1	gRNA bottom strand, 100 uM
1	T4 PNK
1	T4 Ligation Buffer, 10X
6	ddH_2O
10	**Total**

Temperature	Time
37 °C	30 min
95 °C	5 min
Ramp to 25 °C	5 °C/min

Then the annealed, phosphorylated oligos were diluted 1:200 into ddH2O, and stored at -20 °C. The pSpCas9(BB) plasmid (Addgene #62988) was digested with BbsI enzyme under the following conditions:

Amount (uL)	Component
x	pSpCas9(BB), 1 ug
1	BbsI
5	Buffer 2.1
1	CIP
to 50	ddH_2O
50	**Total**

Temperature	Time
37 °C	2 hr

The digested product was run on 1% (wt/vol) agarose gel to visualize digested vector. Then gel extract and product purification was stored at -20 °C. The digested vector backbone (BB) and annealed, phosphorylated oligo insert (gRNA) was then ligated together under the following conditions:

Amount (uL)	Component
2	T4 Ligation Buffer, 10X
1	T4 DNA Ligase
0.5	pSpCas9(BB) vector
3	gRNA
13.5	ddH_2O
20	**Total**

Temperature	Time
16 °C	Overnight

Following ligation, we treated the reaction with PlasmidSafe Exonuclease to remove any residual liner DNA under the following conditions:

Amount (uL)	Component
11	Ligation Reaction
1.5	PlasmidSafe Buffer, 10X
1.5	10 mM ATP
1	PlasmidSafe Exonuclease
15	**Total**

Temperature	Time
37 °C	30 min
70 °C	30 min

Transformation of chemically competent Stbl3 E. coli was performed using the heat shock method. Two uL of plasmid was added to 20 uL cells, mixed and incubated on ice for 30 minutes. Heat shock was performed at 42 °C for 30 seconds and E.coli were immediately returned to ice for 2 minutes. Then we added 600 uL SOC medium to the mix and incubated at 37 °C (shaking) for 1 hour. Then cells were pelleted at 4000 rpm for 2 minutes to remove all but 100 uL of media, followed by resuspension and plating onto LB+ampicillin (100 ug/mL) plates overnight at 37 °C. Inspection for colony growth was performed the next day. We inoculated several colonies into LB + ampicillin (100 ug/mL) and grew them at 37 °C (shaking) overnight. Before harvesting for DNA extraction, we

streaked cultures onto an LB+ampicillin (100 ug/mL) grid plate to retain correct clones. Then we prepared miniprep of the plasmid DNA according to the QIAprep spin miniprep kit instructions. After sequence verification, maxiprep was prepared using Qiagen EndoFree Maxiprep Kit.

To transfect the Cas9-gRNA encoding plasmid by nucleofection, we pre-treated hiPSCs in iPS media containing 10 uM Y-27632 (ROCK inhibitor) for 3 hours before transfection. Then cells were dissociated using Accutase for 5-7 minutes to attain a single cell suspension. Cells were passed through a 30 um strainer to remove cell clumps. Cells were spun at 200 x g for 4 minutes. Then cuvettes were prepared with cells and plasmid DNA mixture (2 ug Cas9/gRNA, 3 ug donor plasmid). After spinning and aspiration of supernatant, we added 100 ul P3 Solution+Supplement (Lonza) per cuvette to the cell pellet. Next using the Amaxa Nucleofector, we transfected the cells using CB-150 program. Then cells were incubated overnight at 37 °C, 5% CO2/5%O2 to allow cells to attach. Twenty-four hours later, media was replaced with fresh media without Y-27632. Then colonies were picked after being challenged with Puromocyn. Surviving colonies were picked into 12-well plates, expanded and PCR screening of gDNA was performed to identify successfully targeted clones. After choosing colonies that were potentially successfully targeted with the corrected BMPR2 template, we Cre-excised the intronic, floxed Puromycin resistance cassette, by transient transfection of plasmid Cre-IRES-NeoR as described before in making hiPSCs section. Successful targeting, BMPR2 mutation correction, and excision of the PuroR cassette was confirmed by both PCR of gDNA and sequencing of the BMPR2 locus (see table 3 for primers.)

Table 3: Primers used for PCR to verify the correction

Primers	Sequence	Binding sites
BMPR2 cDNA	**Forward:** GATCCGTATCAGCAAGACCTTGGG **Reverse:** CAACTGGACGCTCATCCAAGGAGC	**Forward:** 88,535 .. 88,558 **Reverse:** 114,375 .. 144,398
BMPR2 cDNA sequencing	GCTCGAAAGGTAGCACCTGCTATG	88,602 .. 88,625
BMPR2 Integrity of Target site	**Forward:** TGTTGATTTGCAAAACTGTTTCATAGC **Reverse:** ACAGGCGCCTACCACTACGCCCGG	**Forward:** 91,078 .. 91,104 **Reverse:** 93,419 .. 93,442
BMPR2 Family 14 mutation sequencing	GATTTATAGGATGTTGGTCTCACATTG	91,201 .. 91,227
3' Know-in	**Forward:** GCCAGAGGCCACTTGTGTAGCGCCAAG **Reverse:** CACTGCAGTAAACAACTCAAT	**Forward:** 93,040 .. 93,066 **Reverse:** 94,136 .. 94,156

CHAPTER III: RESULTS

3.1 Two stages of directed differentiation of hiPSCs into mesodermal progenitors with endothelial cells competence.

Prasian et al published a 12 day serum-free, feeder-free, two dimensional, monolayered protocol to derive endothelial colony forming cells (ECFC) from hiPSC using four factors, Activin-A (for 24 hours only), BMP4, FGF2 and VEGF. This protocol resulted in the generation of ECFC that were similar to cord blood (CB) ECFC in their endothelial marker expression profile, high proliferative potential, and the ability to form functional blood vessels in vivo (78). To test our first hypothesis, we chose this protocol as a model to investigate the kinetics of hiPSC differentiation and whether the cells are differentiating through stages that recapitulate those that are involved in embryonic endothelial cells development. To improve the reproducibility of the protocol, we applied the following changes: 1) differentiation of dispersed, adherent cells plated in 2D as single cell suspensions instead of colony based 2D differentiation, 2) cells were passaged by day 4, 3) seeding cell density at day-2 and day4 was optimized for each cell line**.** To investigate the kinetics of the differentiation protocol, we looked at protein and gene expression for primitive streak (T), endoderm (FOXA2), mesoderm (KDR), lateral plate mesoderm (FOXF1), paraxial mesoderm (TBX6), intermediate mesoderm (PAX2) and endothelial (KDR, CD31 and CD144) markers by FACS analysis and RT-qPCR at different time points. FACS analysis shows 28.8% of differentiating cells express cell surface marker for mesoderm; KDR, by day4 and by day12 this percentage increases to almost 100%. By Day12, 7% of the cells express cell surface markers for endothelial cells (CD31 and KDR), these cells were sorted, replated and maintained in EGM-2/BFV media. FACS analysis of the sorted cells at day24 (Day12 post sort) shows 92% of the

cells express CD31 and CD144, indicating the possibility of generating endothelial-like cells by that time based on expression of endothelial cells surface markers (CD31 and CD144) only at this stage **(Figure-1 B)**.

Gene expression kinetics by RT-qPCR of unsorted cells undergoing directed differentiation shows a transition through a primitive streak stage characterized by transient brachyury (T) expression that peaks by day 2 to a mesoderm stage indicated by expression of mesodermal markers: KDR, FOXF1, PAX2 and TBX6). Note the heterogeneous nature of the mesoderm produced by day 4, including the generation of cells expressing markers of lateral plate (FOXF1), intermediate (PAX2,) or paraxial mesoderm (TBX6). By day 8-12 the protocol promotes lateral plate mesodermal marker (FOXF1) expression at the expense of expression of intermediate mesoderm. Note also the transient expression of low levels of anterior primitive streak (non-mesodermal) marker (FOXA2) within the first 4 days of the protocol and its downregulation by day 4 of the protocol, indicating the absence of anterior primitive streak or endodermal cell outgrowth in days 4-12 of this protocol **(Figure-1 C)**.

It can be concluded from the kinetic experiments, that BMP4, FGF2 and VEGF (with Activin for 24hrs), promotes the differentiation of hiPSCs through stages that recapitulate those involved in the embryonic derivation of endothelial cells, in which cells progress through a primitive streak-like state (T+) to mesoderm and subsequently to a population of cells 90% of which express endothelial cell surface markers (CD31, CD144 and KDR), indicating the possibility of generating potential endothelial-like cells.

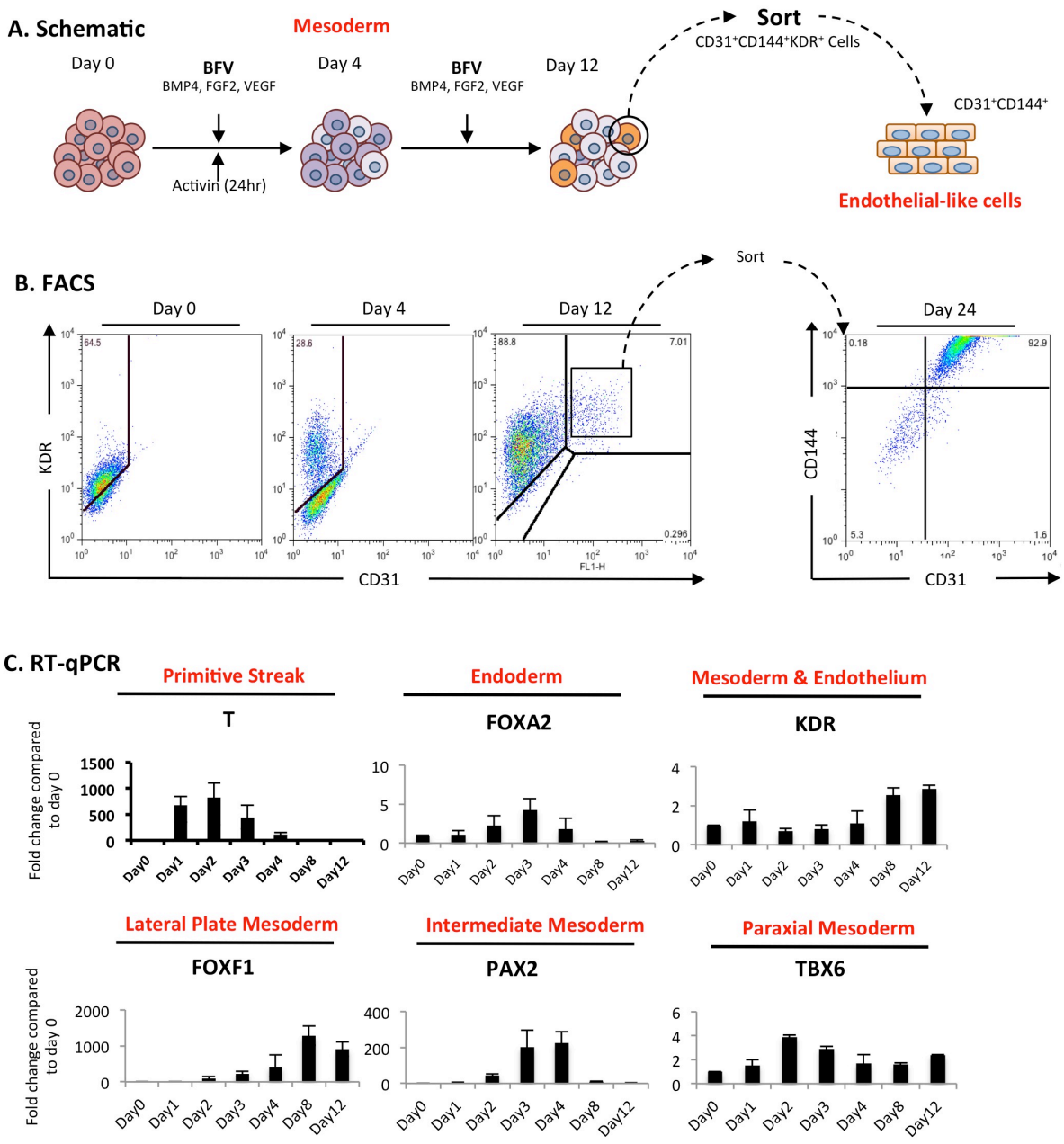

Figure 1: Two stages of directed differentiation of hiPSCs into mesodermal progenitors with EC competence

A. Schematic of feeder free, serum free two-stage differentiation protocol for the directed differentiation of hiPSC into endothelial colony forming cells with high proliferative potential.

B. Kinetics of cell surface KDR and CD31 protein expression, at indicated stages of differentiation. After sorting by day 12, 92% of cells express CD31 and CD144 and can be serially passaged.

C. Gene expression kinetics by RT-qPCR of unsorted cells undergoing directed differentiation through the 2 stage protocol, indicating progression through a primitive streak stage characterized by transient brachyury (T) expression that peaks by day 2 to a mesoderm stage indicated by expression of the mesodermal markers: KDR, FOXF1, PAX2 and TBX6.) Note the heterogeneous nature of the mesoderm produced by day 4, including the generation of cells expressing markers of lateral plate (FOXF1), intermediate (PAX2,) or paraxial mesoderm (TBX6). By day 8-12 the protocol promotes lateral plate mesodermal marker (FOXF1) expression at the expense of expression of intermediate mesoderm. Note also the transient expression of low levels of anterior primitive streak (non-mesodermal) marker (FOXA2) within the first 4 days of the protocol and its downregulation by day 4 of the protocol, indicating the absence of anterior primitive streak or endodermal cell outgrowth in days 4-12 of this protocol.

3.2 Differentiation of iPSCs yields an endothelial-like population that maintains high proliferative potential and expression of endothelial cell surface markers over several passages.

To investigate the phenotypic and functional characteristics of the generated cells and whether they resemble ECFC, we used several known characterization assays to test: 1) proliferative capacity, 2) expression of endothelial markers, 3) morphological characteristics, and 4) ability to form functional blood vessels in vivo.

To assess the proliferative potential of the sorted $CD31^{+}CD144^{+}KDR^{+}$ cells, they were plated at low density (600 cells/cm2) in a 12-well plate. As cells attach and form colonies, the cell number composing single colony (several colonies were chosen randomly) was counted at different time points. Over 11 days (post-sort; total differentiation day 23), our results show a range of increases in cell numbers in different colonies, ranging from 11 to 90 fold increases over input numbers, indicating that this differentiation protocol yielded endothelial-like cells with variable proliferative potential **(Figure 2)**.

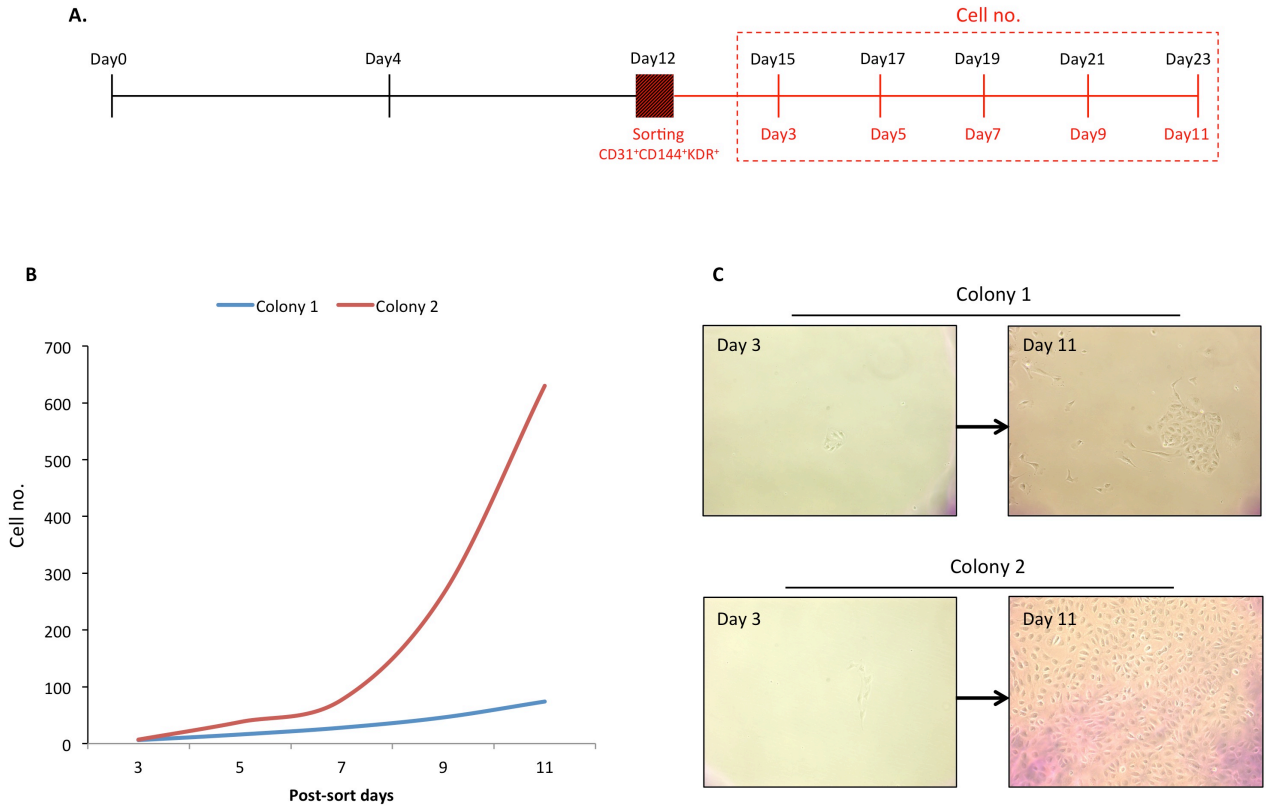

Figure 2: sorted $CD31^{+}CD144^{+}KDR^{+}$ cells derived from hiPSCs produce colonies with variable proliferative potentials

A) Schematic indicating the post-sorting time points, in which the numbers of cells were counted

B) Line chart showing the proliferation of two colonies of the sorted $CD31^{+}CD144^{+}KDR^{+}$ cells over 11 days post sort. These results show that colony 1 had 11 fold increase in the cell number over 11 days, while colony 2 had a 90 fold increase. These results indicate that different colonies had different proliferation potentials.

C) Microscopic images showing the increase in cell number over 11 days post sort.

One of the characteristics of ECFC is the expression of endothelial cell markers and their ability to proliferate for extended periods of time in vitro without drifting to non-endothelial phenotypes. To assess the expression of endothelial markers after passaging sorted $CD31^{+}CD144^{+}KDR^{+}$ cells, RT-qPCR and FACS were performed. The results show similar protein and transcript gene expression levels of endothelial markers (CD31 and CD144) between the sorted cells and CB-ECFC **(Figure-3 A, B)**. To confirm the expression of endothelial markers, we immunostained the sorted $CD31^{+}CD144^{+}KDR^{+}$ cells for CD31 and NRP-1, and results show typical cobblestone morphology and protein expression pattern of CD31 and NRP-1 of the sorted cells as endothelial cells **(Figure-3 C)**. Hence our results show that the sorted cells maintained the expression of endothelial cell surface markers (CD31 and CD144) over 8 passages, indicating the maintenance of phenotype based at least on markers expression **(Figure-3 B)**.

Endothelial cells are characterized by being able to uptake acetylated low density lipoprotein (Ac-LDL). To assess the ability of sorted iPSC-derived $CD31^{+}CD144^{+}KDR^{+}$ cells to show similar characteristics, they were incubated with media containing Dil-Ac-LDL for 2 hours, and microscopic images were taken. These images reveal that sorted cells were positive for Ac-LDL uptake **(Figure-3 D)** similar to endothelial cells (data not shown).

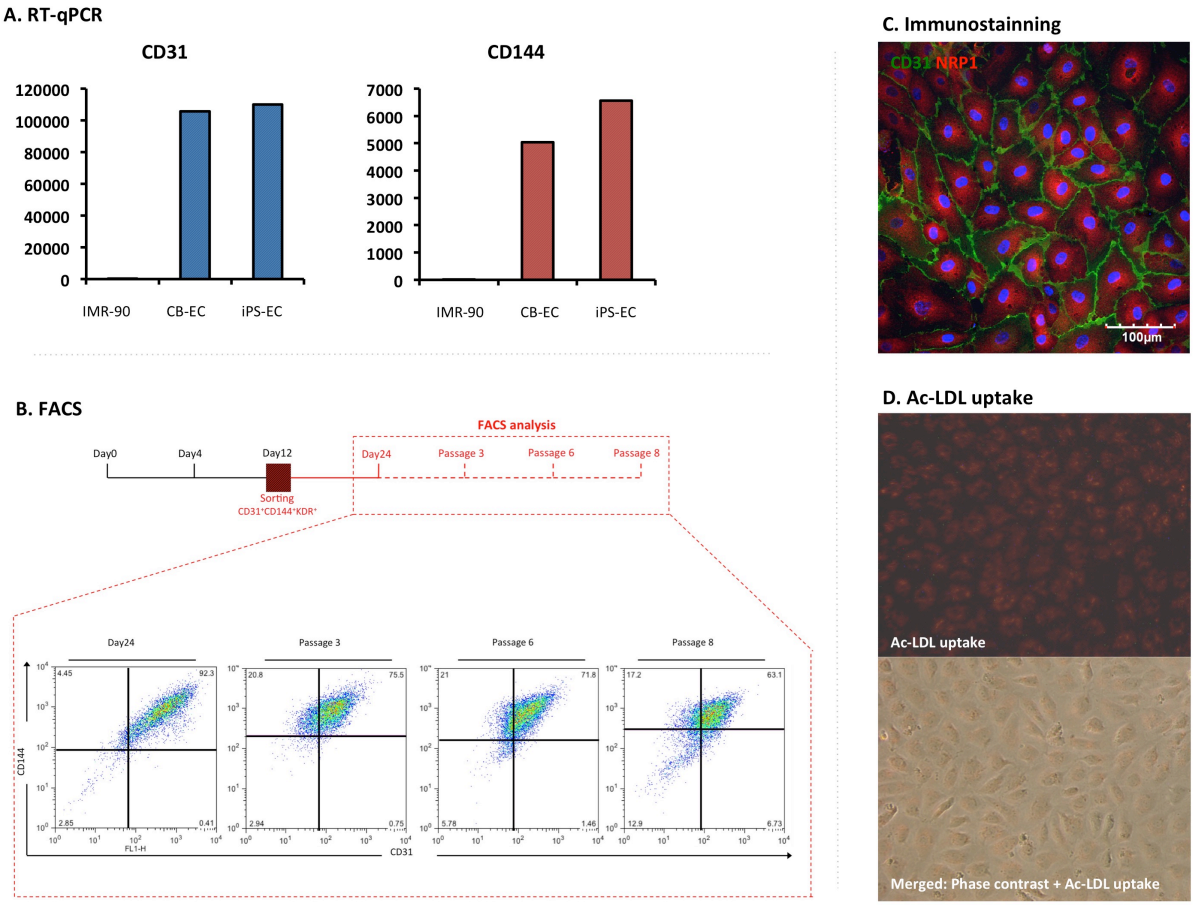

Figure 3: The sorted $CD31^{+}CD144^{+}KDR^{+}$ express and maintain endothelial markers over 8 passages

A) RT-qPCR showing similar gene expression level of endothelial markers (CD31 and CD144) of the sorted $CD31^{+}CD144^{+}KDR^{+}$ with CB-ECFC.

B) FACS plot showing that the sorted $CD31^{+}CD144^{+}KDR^{+}$ cells expressing and maintain endothelial markers over 8 passages.

C) Immunostainning showing of the sorted $CD31^{+}CD144^{+}KDR^{+}$ cells, showing typical cobblestone morphology and expression of CD31 and NRP-1

D) AC-LDL uptake assay was positive for the sorted $CD31^{+}CD144^{+}KDR^{+}$ cells

Another characteristic of endothelial cells is their ability to form network structures in in vitro matrigel assays. To investigate the ability of the sorted $CD31^{+}CD144^{+}KDR^{+}$ cells to form similar network structures to ECFCs, Sorted iPSC-derived putative ECs, vs CB-ECFC and IMR-90 fibroblast positive and negative controls, respectively, were plated on 96-well plates pre-coated with thick matrigel. After 16 hours, images were taken and analyzed using ImageJ software with AngioAnalyzer plug-in. Results show that both CB-ECFC and iPS-EC formed similar number of branches, segments, connecting segments and meshes in comparison to the negative control; IMR-90 **(Figure 4)**. Note that as the structures become more complex, CB-ECFC performed better than iPS-EC. These results indicate that the sorted cells were able to form network-like structure but were performed less than CB-ECFC, as the complexity of the structure increase.

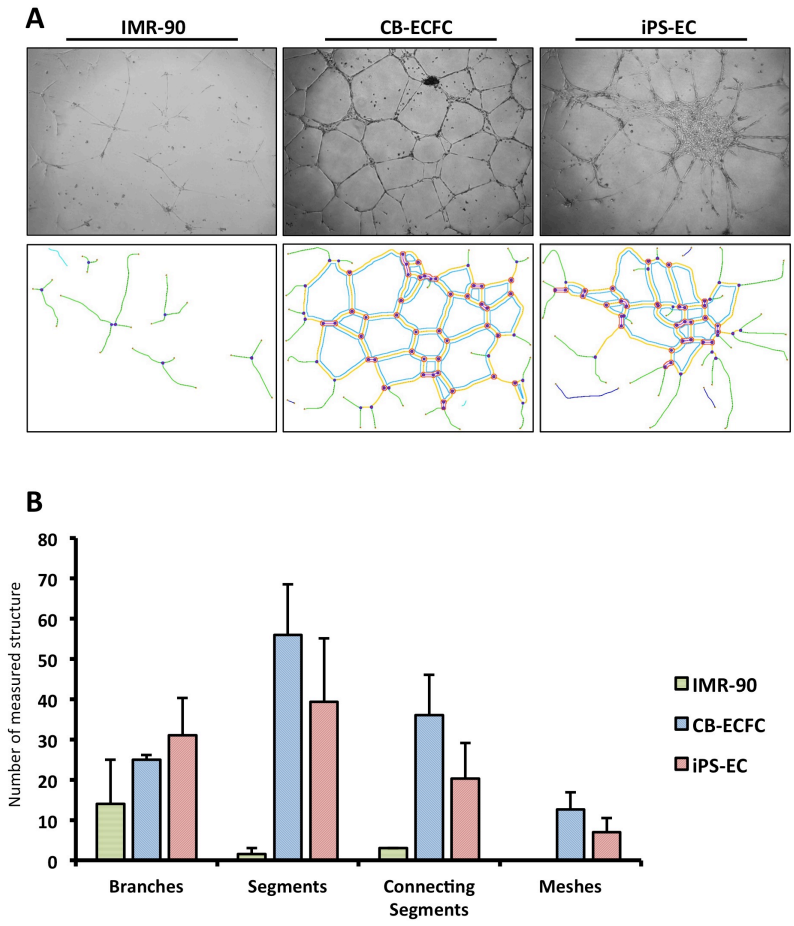

Figure 4: The sorted $CD31^{+}CD144^{+}KDR^{+}$ were able to form network like structure in in vitro matrigel assay, but was less complex than CB-ECFC

A) Microscopic images (Top panel) of in vitro matrigel assay for the sorted $CD31^{+}CD144^{+}KDR^{+}$ cells, CB-ECFC and IMR-90. Lower panel shows computed images generated with ImageJ.

B) Bar graph showing the number of structures created by each cell type, calculated through automated plug-in in ImageJ.

In order to test the ability of iPS-EC to form functional blood vessels in vivo, cells were sent to our collaborators (Laboratory of Dr. Mervin C. Yoder, Indiana University) to prepare Matrigel plugs containing iPSC-derived EC (iPS-EC). These plugs were implanted subcutaneously in SCID mice. After 24 days following transplantation, the plugs were harvested by dissection, fixed with paraformaldehyde, and tissue sections were prepared for histology studies including immunostainings with anti-human CD31 antibody **(Figure 5)**. iPS-EC were able to survive the in vivo assay and able to form tube-like structures that were stained with anti-human CD31 antibody. However in comparison to CB-ECFC, iPS-EC failed to form tube-structures that enclose circulating red blood cells, indicating that these tubes failed to anastomose with host vasculature and therefore were not able to function as vessels compared to the primary CB-ECFC controls **(Figure 5)**.

It can be concluded from the several in vivo and in vitro characterization assays, that this directed differentiation protocol yields an endothelial like population, a subset of which were able to maintain high proliferative potential and expression of endothelial cell surface markers for at least 8 passages. Although the cells engineered from iPSCs possess other endothelial cell characteristics, such as the capacity to take up Ac-LDL, and form tube-like structures in 3D matrigel they are not functionally identical to CB-ECFC in vivo.

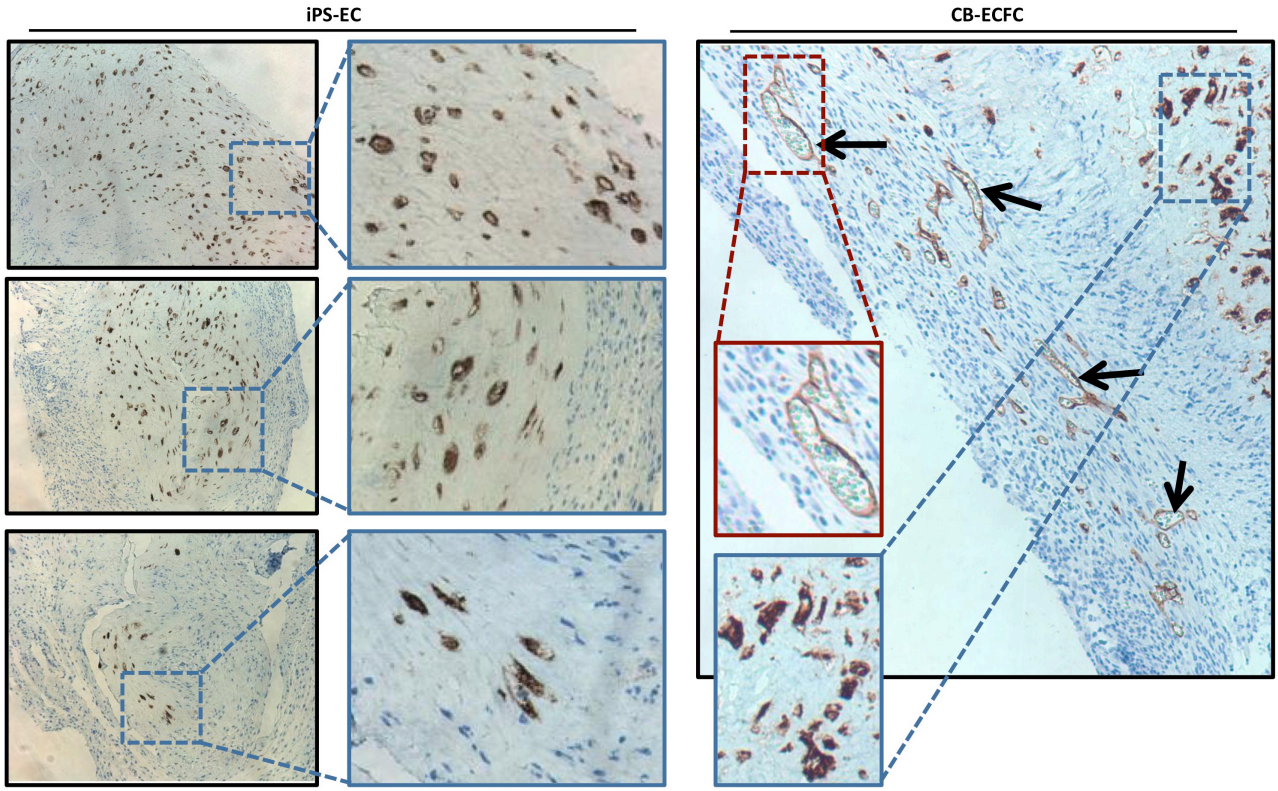

Figure 5: Sorted CD31^{+}CD144^{+}KDR^{+} cells derived from iPSCs were able to survive and make tube like structure in vivo, but failed to harbor blood cells in comparison to CB-ECFC controls.

Histological sections of Matrigel plugs that were seeded with sorted CD31^{+}CD144^{+}KDR^{+} cells or CB-ECFC and implanted in SCID mice. The images show that the sorted CD31^{+}CD144^{+}KDR^{+} cells were able to form tube like structures positive for human-specific CD31 by immunostaining, but devoid of any circulating blood cells, indicating that these tubes did not anastomose with the host vasculature. In contrast CB-ECFC sections show two types of tube like structures: those that harbor blood cells (Black arrow and red-box) and those that do not (Blue-box). Note blue box structures appear similar to those formed by the sorted CD31^{+}CD144^{+}KDR^{+} iPS-ECs.

3.3 BMP4 is necessary and sufficient for the induction of endothelial competent mesoderm but is dispensable for subsequent lineage specification of endothelial like cells.

After developing an in vitro model to differentiate hiPSCs into endothelial like cells, the next step for the project is to test the second hypothesis by using this model to study human vascular development and pathogenesis of vasculopathies such as HPAH. As discussed before, about 80% of HPAH is caused by a mutation in BMPR2. While BMPR2 mutations are present in every cell in the body and BMPR2 protein is expressed in a wide variety of tissues and cell types, it is unknown why only the pulmonary vasculature shows clinically apparent abnormalities. It is also unknown whether there is a developmental abnormality in lung-specific endothelial cells. Our in vitro differentiation model depends on BMP4, which is one of the ligands of BMPR2 used to derive ECs from hiPSCs, therefore it is possible to use this model to investigate the role of BMP signaling in the derivation of endothelial cells in vitro and to begin to develop and in vitro disease model.

To study the role of BMP signaling in EC derivation from hiPSCs, we first sought to determine the stage dependent requirements for exogenous BMP4 in our two staged protocol. We designed an experiment **(Scheme 3)** in which BMP4 was used as the only differentiating factor, or was withdrawn or blocked using the BMP antagonist, Noggin, at the induction (Day0-4) and/or specification (Day4-12) stages of the protocol. Description of conditions is shown in Table 4. FACS analysis and gene expression by RT-qPCR were performed on day 4 and day12.

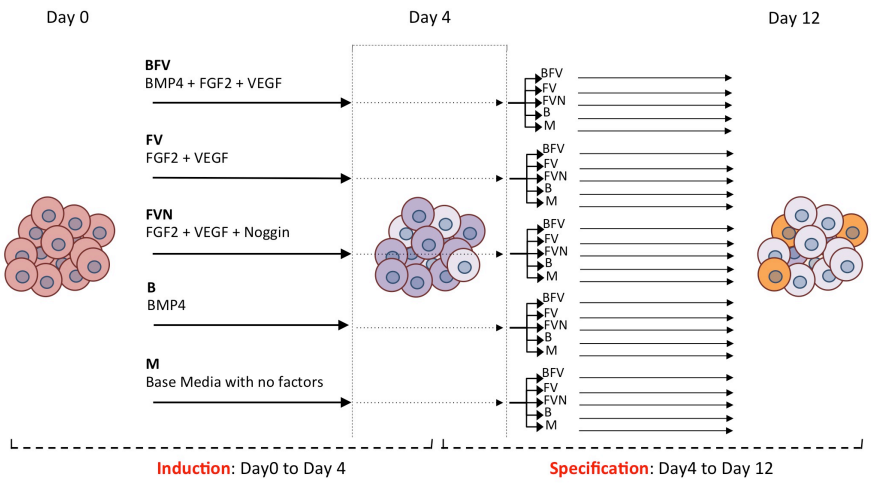

Scheme 3: Schematic summarizing the media abbreviations and combinations tested for induction and specification stages of the protocol.

Table 4: Medium's components for different conditions

Name	Components
M	Base media with no factors added
BFV	Base media with BMP4, FGF2 and VEGF
FV	Base media with FGF2 and VEGF
B	Base media with BMP4 only
FVN	Base media with FGF2, VEGF and BMP inhibitor Noggin

Note that all conditions had Activin for the first 24 hours

Day4 FACS analysis shows that conditions lacking BMP4 (M, FV and FVN), result only in KDR^{+dim} cells, while while conditions that contain BMP4 (B and BFV) induce two distinct populations: $KDR^{+bright}$ and KDR^{-} cells, similar to our results using all factors (BFV) **(Figure 6)**. Day12 FACS analysis shows that CD31+CD144+ cells only arise from those conditions that were exposed to BMP4 at the induction stage (day0-4) and from those conditions that contain FGF2 and VEGF at the specification stage (day4-12). These FACS results indicate that BMP4 in this protocol is required for inducing mesodermal cells with endothelial competence, but is not required for specifying them toward endothelial cells lineages. However the opposite is true for FGF2 and VEGF: while they are not required for inducing the endothelial competent mesodermal cells, they are necessary for lineage specification into endothelial cells.

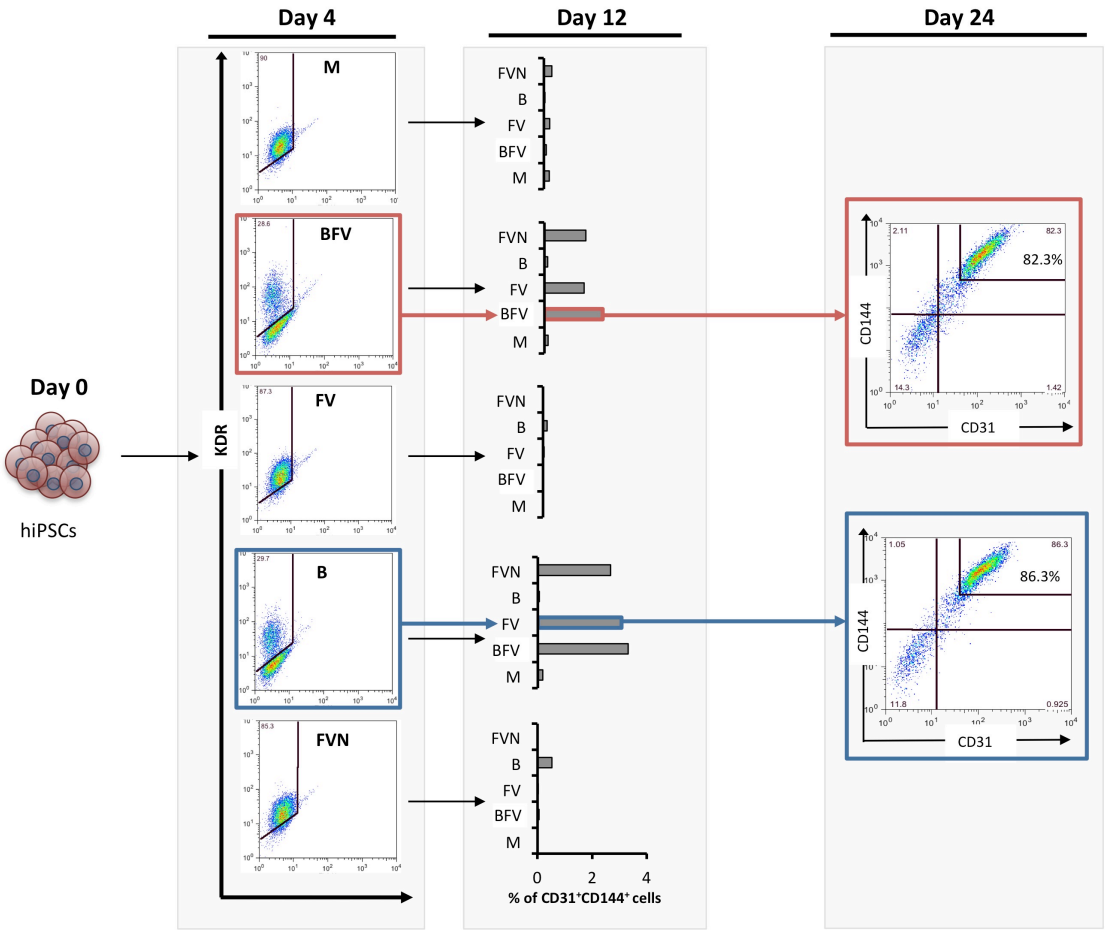

Figure 6: Stage-dependent BMP4 is necessary and sufficient for the induction of endothelial competent mesoderm but is dispensable for subsequent lineage specification of endothelial-like cells.

Panels on the left are FACS plots of day 4 cells differentiated in the conditions indicated from day 0-4 (all conditions include day 0-1 exposure to Activin). (M = base media with no factors added, B = BMP4 only, BFV = BMP4, FGF2 and VEGF, FV = FGF2 and VEGF, FVN = base media with FGF2, VEGF and the BMP inhibitor, Noggin). Note the 2 distinct populations of KDR^{high} and KDR^{-} cells are present only in those two conditions that contain BMP4. The middle panel is a bar graph representing the % of CD31+CD144+ cells by FACS on day12 (after day 4-12 culture in each indicated media cocktail). CD31+CD144+ cells arise only from those precursor cells that were patterned in BMP4-containg conditions (B or BFV from day0-day4.) The right panel is a FACS plot of day24 cells. These cells were sorted at day 12 after being induced by either B or BFV at the induction stage, then specified by either FV or BFV. The similar percentage of CD31+CD144+ cells, supports the conclusion that BMP4 is necessary and sufficient at the induction stage but is dispensable at the specification stage.

To confirm the FACS results, we performed RT-qPCR for cells exposed to BFV, FV and B conditions at each day during the induction stage (Day0-4) to define the kinetics of gene expression of primitive streak (T), endoderm (FOXA2), mesoderm (KDR), lateral plate mesoderm (FOXF1), paraxial mesoderm (TBX6) and intermediate mesoderm (PAX2). All conditions had Activin for the first 24 hours. The results show that cells which exposed to FV had low expression of primitive streak (T), lateral mesoderm (FOXF1) and intermediate mesoderm markers (PAX2) and up regulation of endoderm marker (FOXA2) and paraxial mesoderm marker (TBX6) over the 4 days of induction. In contrast, those cells which were exposed to B and BFV conditions show transient upregulation of primitive streak marker (T), upregualtion of lateral plate and intermediate mesoderm (FOXF1 and PAX2 respectively) and low expression of endoderm and paraxial mesoderm marker (TBX6) over 4 days of induction **(Figure 7 A)**. The gene expression kinetics results show that cells proceed through primitive streak stage and subsequently to lateral and intermediate mesoderm stage only in those conditions that contain BMP4 (B and BFV). These results indicate BMP4 is required to induce the cells to differentiate through primitive streak stage to lateral and intermediate mesoderm while both exogenous FGF and VEGF is dispensable. In support of this conclusion day 4 gene expression level of cells exposed to the FV condition or to conditions with no exogenous factors (M), were similar for all tested markers (T, FOXA2, FOXF1, PAX2 and TBX6), indicating that at least for the tested markers, FV and VEGF had no significant differentiation effect during the induction stage **(Figure 7 B)**. Similar experiments were done during the specification stage, in which the cells that were exposed to conditions that contain BMP4 (B and BFV) were exposed to BFV or FV conditions to investigate if BMP4 is required during the specification stage, and Day 12 RT-qPCR results show similar gene expression of mesoderm markers (KDR, FOXF1, PAX2 and TBX6) and

endothelial markers (KDR and CD31) in conditions regardless of whether BMP4 is present on days 4-12. This indicates that BMP4 is dispensable at the specification stage **(Figure 7 C)**.

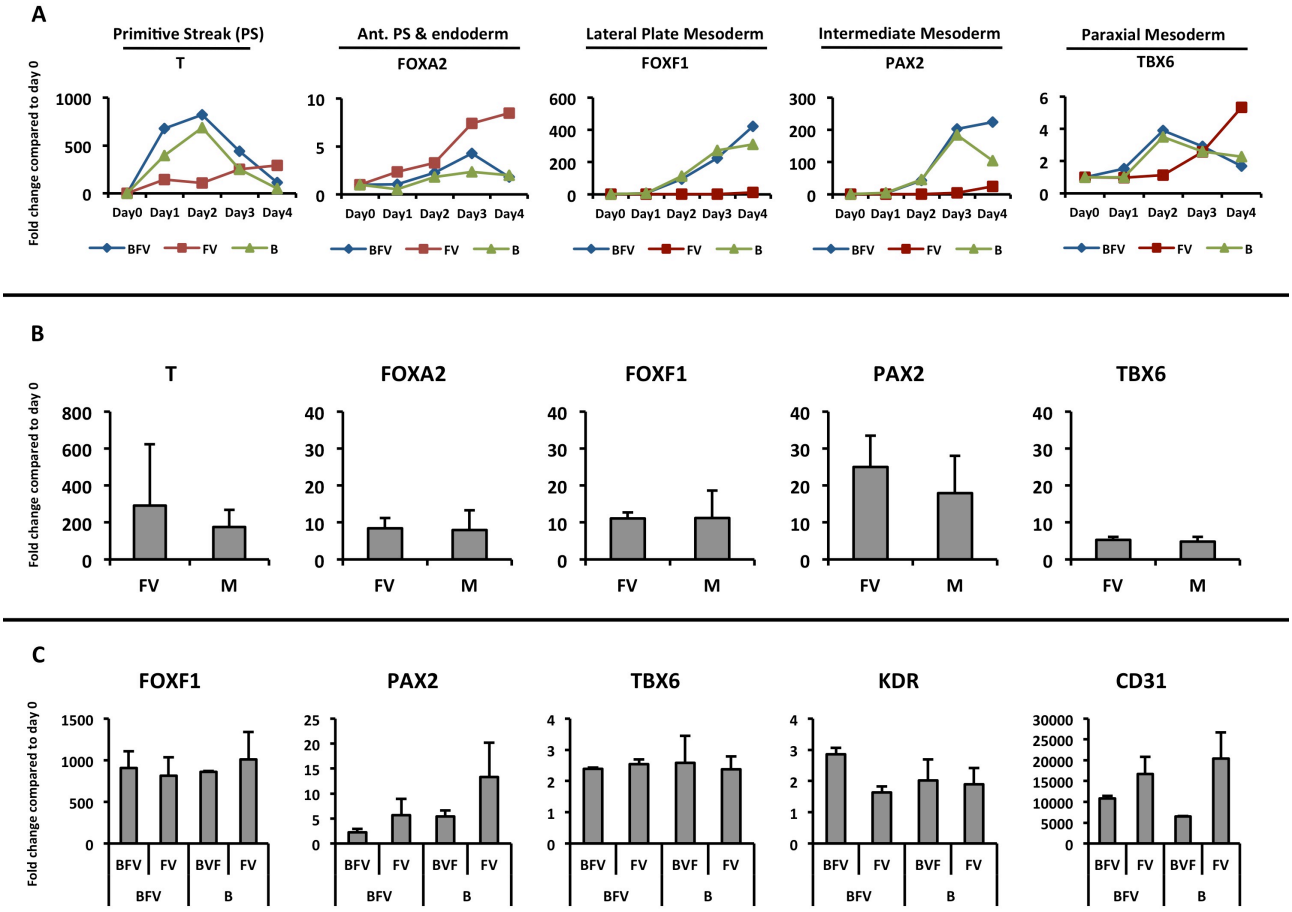

Figure 7: In contrast to BMP4, FGF and VEGF do not promote the differentiation of pluripotent stem cells through primitive streak to mesodermal stage cells.

A) Line graph showing kinetics of gene expression (by RT-qPCR) of primitive streak (T), endoderm (FOXA2), mesoderm (KDR), lateral plate mesoderm (FOXF1), paraxial mesoderm (TBX6) and intermediate mesoderm (PAX2) markers at the induction stage and with three conditions (BFV, B, or FV).

B) Bar graph showing a comparison of gene expression by hiPSCs that were exposed to FV or M at the induction stage.

C) Bar graph showing a comparison of gene expression by hiPSCs that were exposed to BFV or FV at the specification stage, after being induced by either BFV or B conditions.

It can be concluded that in this in vitro differentiation model, BMP4 is necessary and sufficient for the induction of endothelial competent mesoderm but is dispensable for subsequent lineage specification of endothelial-like cells. On the other hand the opposite is true for FGF2 and VEGF, in which they are required for the specification of endothelial like cells after the induction of endothelial competent mesoderm, but they are dispensable at the primitive streak and mesoderm induction stages. To further validate this conclusion we differentiated hiPSCs in parallel using 2 protocols: 1) the original protocol that used BFV through all 12 days (78) and 2) Our new protocol using B in the first 4 days (induction stage) and FV on days 4-12. On day 12 CD31+CD144+ cells were sorted and replated as described before. At day 24, FACS analysis was done for the sorted cells from both protocols, revealing that both protocols resulted in similar percentages of CD31+CD144+ cells **(Figure 6)**.

To further understand the role of BMP4 in the derivation of the endothelial competent mesoderm, we exposed hiPSCs to BMP4 for different lengths of time (24hr, 48 hours, 96 hours and 120 hours) and then switched to conditions that contain FV and VEGF only till day 12 **(Figure 8 A)**. FACS analysis and RT-qPCR were done at day 4 and 12. The results shows that as little as 24 hours of exposure to BMP4 results in successful induction of primitive streak and mesoderm markers (T, FOXA2, KDR, FOXF1, TBX6, PAX2 and CD31) and percentages of $KDR^{+bright}$ mesoderm and CD31+CD144+ EC-like cells at days 4 and 12, respectively.. It can be concluded from this experiment that 24 hours of BMP4 exposure is sufficient to induce endothelial competent mesodermal cells.

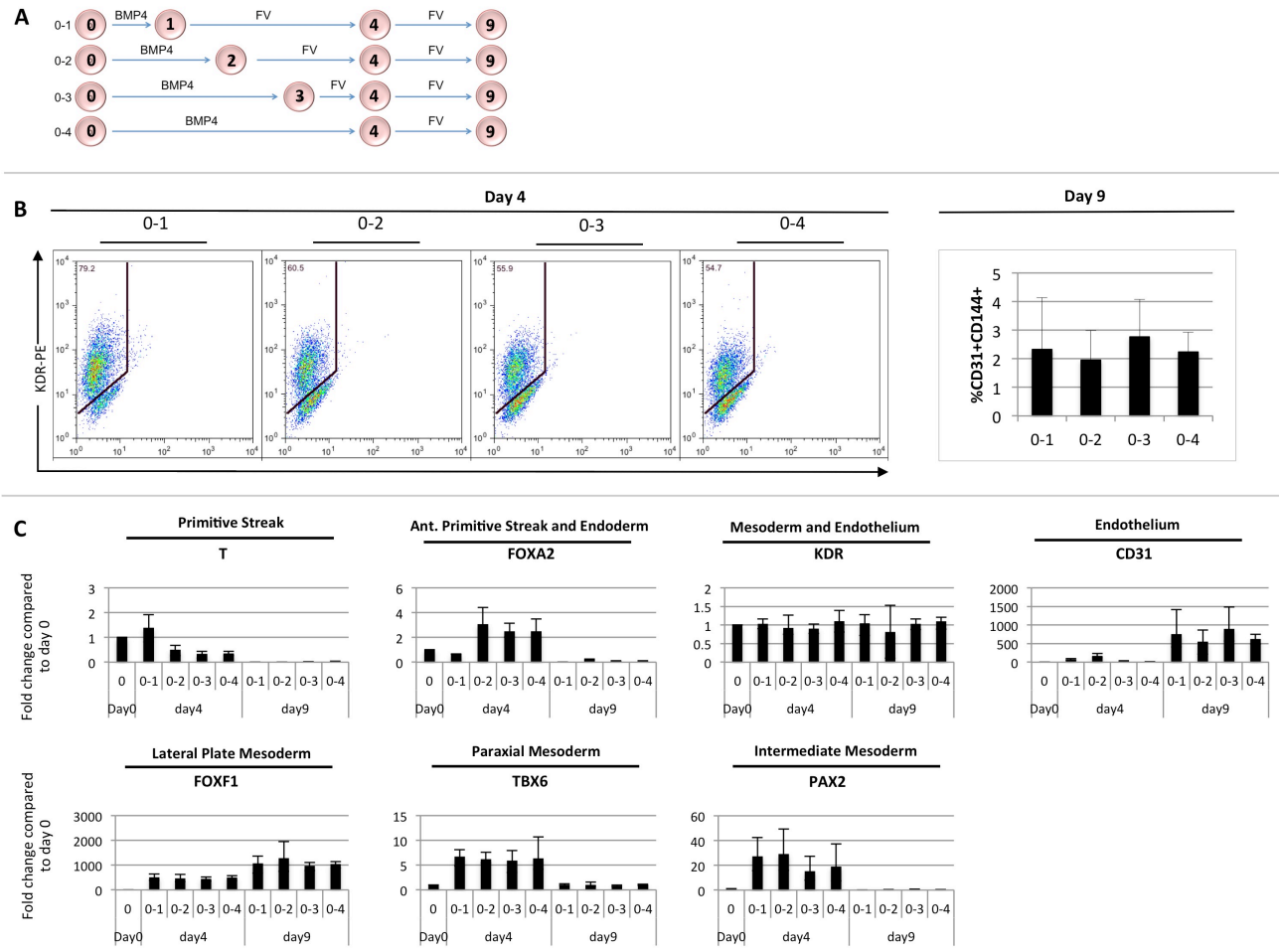

Figure 8: Twenty-four hours of BMP4 exposure is sufficient to induce endothelial competent mesodermal cells.

A) Schematic summarizing the media and combinations tested at different time points.

B) Left panel shows FACS plots of cells exposed to different durations of BMP4. Results show similar percentages of $KDR^{+bright}$ cells are induced by different BMP4 durations. Right panel shows bar graph of percentage of CD31+CD144+ cells on day 12 resulting from precursors exposed initially (days 0-4) to different durations of BMP4.

C) Gene expression of several markers after being induced by different BMP4 exposure times. Results shows that as little as 24 hrs of BMP4 exposure was enough to induce the cells to proceed through PS stage into mesodermal cells with endothelial competence.

3.4 The generated hiPSCs lines from skin fibroblasts isolated from patients with HPAH, have normal karyotypes and their mutations in the BMPR2 gene can be corrected successfully with CRISPR/CAS9 technology.

After developing an in vitro directed differentiation protocol of hiPSCs into endothelial like cells, and achieving a better understanding of the role of BMP signaling in deriving endothelial-like cells, we decided to use this model to test the following hypothesis "The induction of endothelial competent mesoderm is compromised in hiPSCs lines derived from patient with BMPR2 mutations, resulting in insufficient derivation of endothelial-like cells". To test this hypothesis, we planed an experiment **(Scheme 4)** that will consist of: 1) generating hiPSC lines from individuals that carry known BMPR2 mutations and either do or do not have clinical PAH, 2) correcting BMPR2 mutations in all iPS cell lines, 3) differenting all cell lines toward endothelial to assess the role of defective signaling. This approach allows the generation of endothelial-like cells in a head to head syngeneic comparison of iPSC lines both before vs after correction of their BMPR2 mutations by gene editing.

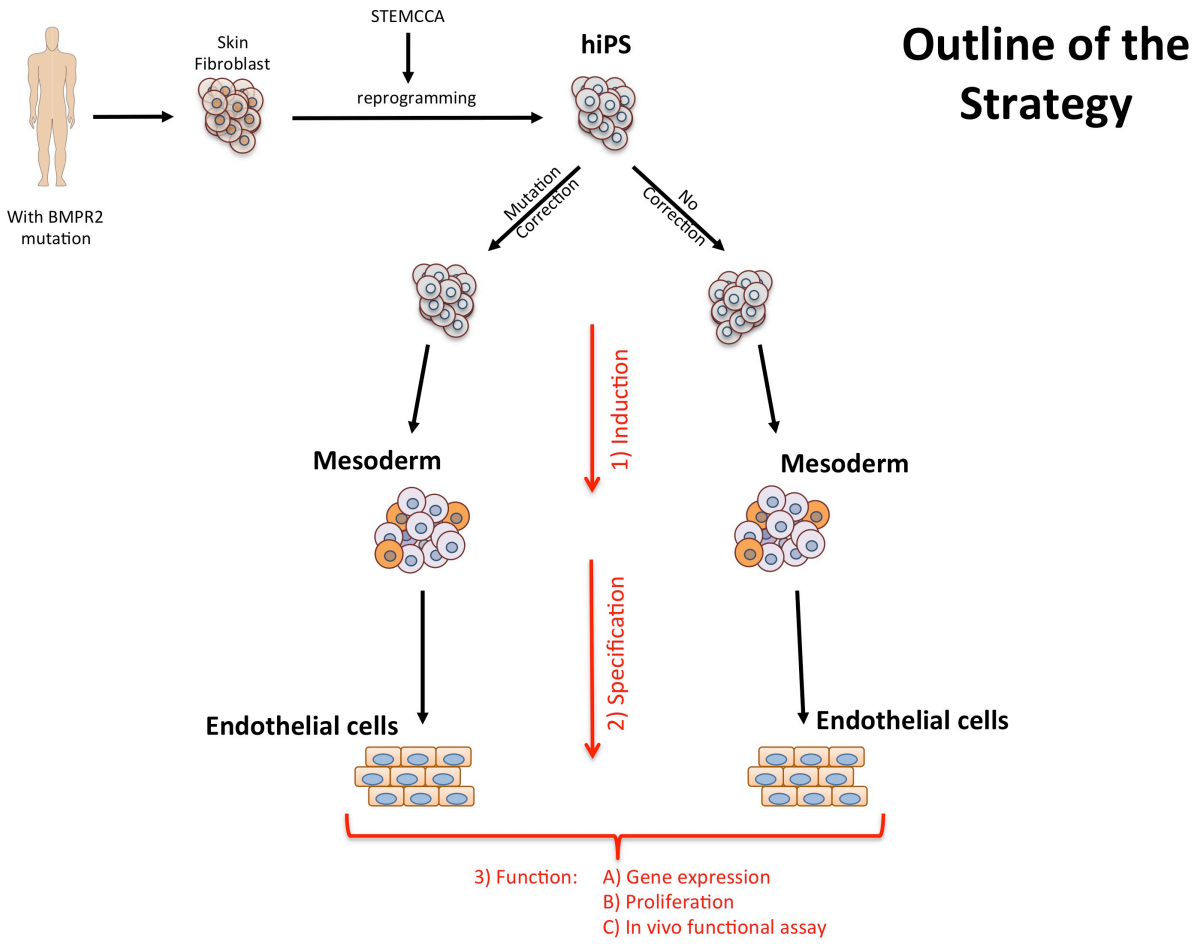

Scheme 4: Schematic of the strategy to test the effect of disturbed BMP signaling due to BMPR2 mutation.

Using the hSTEMCCA reprogramming system (Figure 9 A), we were able to generate hiPSCs from dermal fibroblast that were isolated from patients with HPAH. The generated HPAH1, 2, 3 and 4 hiPSC lines were immunostained with antibodies specific for human pluripotency markers SSEA-4, TRA-1-60 and TRA-1-80. Immunostaining shows that all HPAH-hiPSCs lines were positive for all pluripotent markers (Figure 9 B). After successful reprogramming, we excised the floxed hSTEMCCA vector with transient expression of Cre recombinase and confirmed the excision of STEMCCA by PCR of gDNA (Figure 9 C). G-banding analysis of the generated HPAH hiPSCs revealed normal karyotypes in each gene edited/correct clone as well as their parental clones with no apparent chromosomal abnormalities (Figure 9 B).

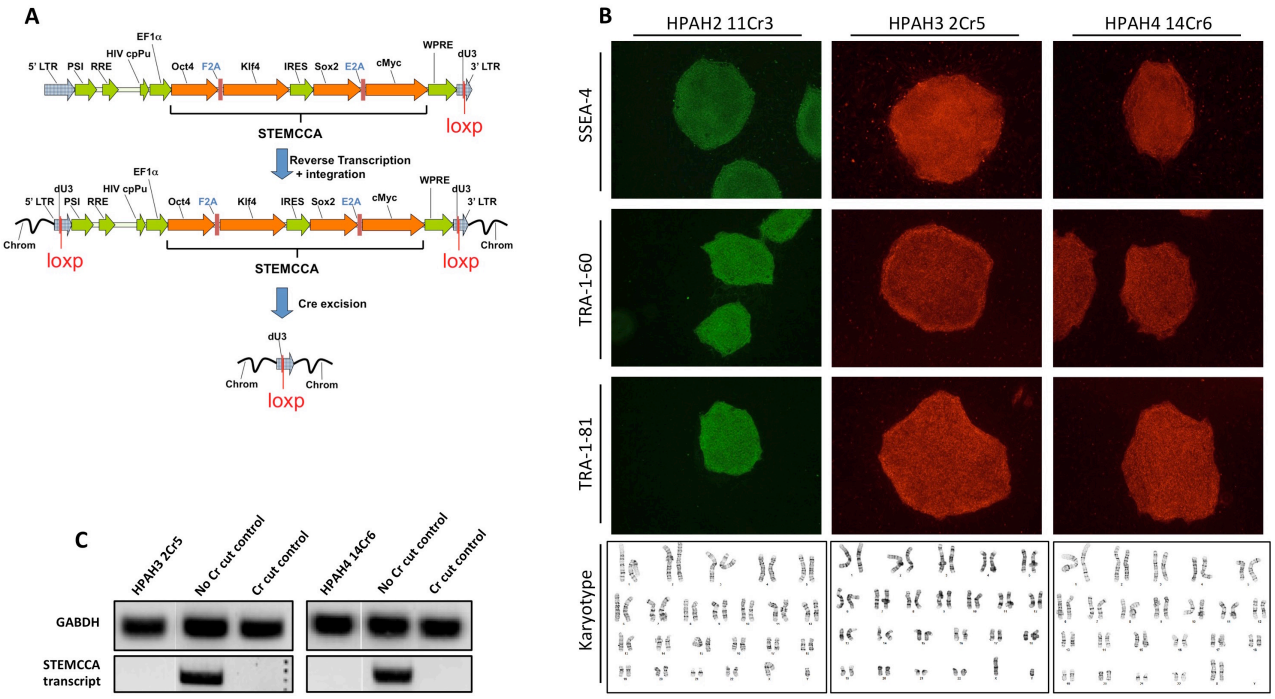

Figure 9: The generated HPAH-hiPSCs show normal karyotype and express pluripotent markers.

A) Vector schematic illustrating the polycistronic lentiviral STEMCCA backbone encoding four reprogramming factors. A loxP site inserted in the viral 3' LTR is duplicated to the 5' LTR during viral infection and reverse transcription. The resulting floxed vector integrated in the host mammalian genome can then be excised by Cre recombinase.

B) Characterization of HPAH hiPSC clones, showing expression of typical pluripotent stem cell markers. Bottom panel shows normal karyotypes of generated HPAH hiPSC clones.

C) RT-PCR showing excision of STEMCCA when compared to non-cut-control

Next we sought to correct the mutation using CRISPR/Cas9 technology. Sequencing data showed that all family 14 HPAH-hiPSCs lines were successfully corrected. (HPAH2, 3 and 4).

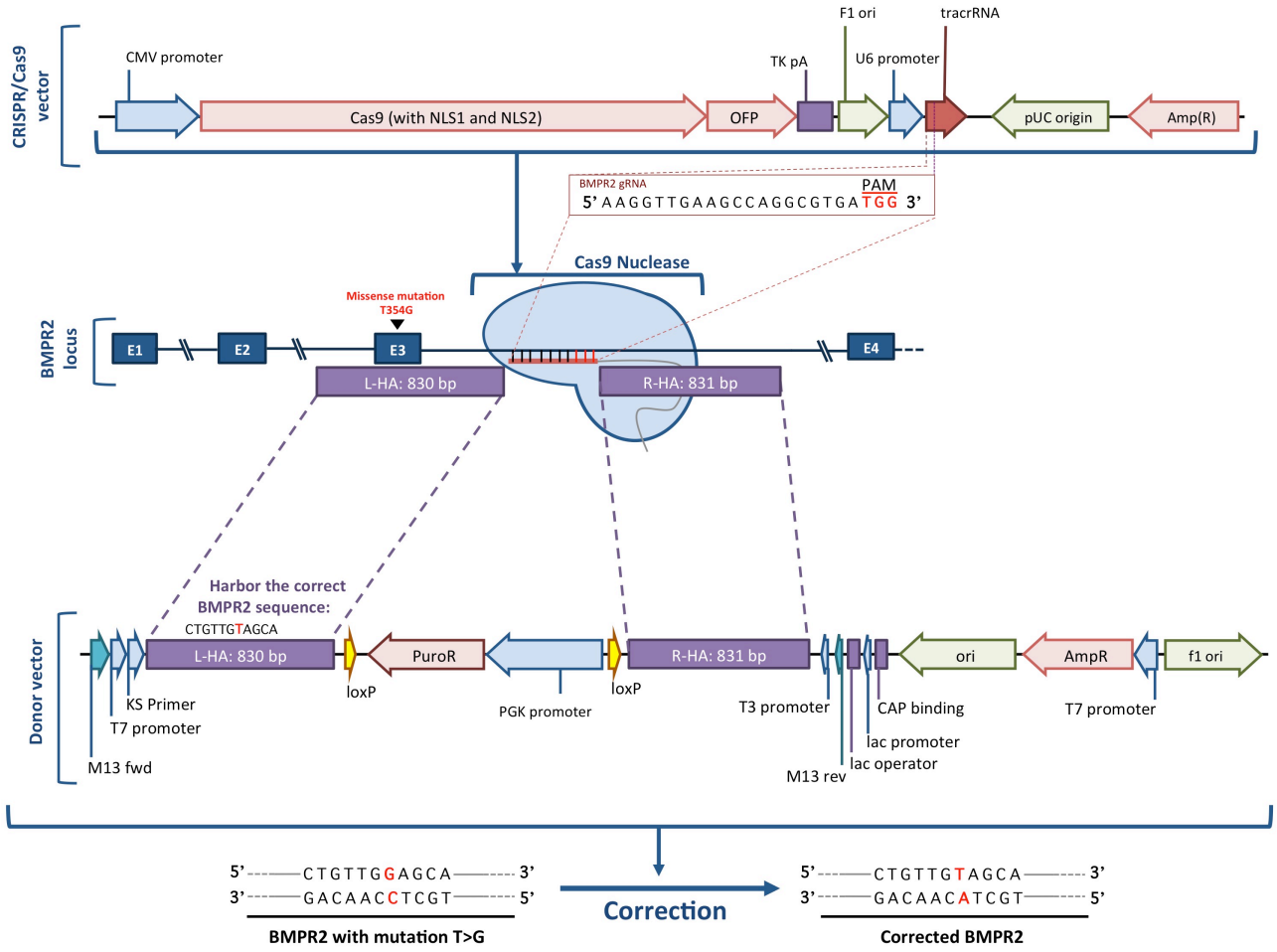

Scheme 5: Schematic of CRISPR/Cas9 correction strategy.

The top panel shows CRISPR/Cas9 vector with the gRNA. The middle shows BMPR2 locus with Cas9 nuclease bind to the intron region downstream of exon 13 guided by gRNA. The bottom panel shows the donor vector with corrected sequence of BMPR2 within the left homology arm, loxP site (for cre-excision) and PuroR-cassette for selection.

After correcting the BMPR2 mutation in each line we performed two pilot experiments. First, we differentiated both HPAH1 and 100-3 iPSC lines using our in vitro differentiation protocol, and investigated the induction of $KDR^{+bright}$ cells by day 4 and the percentage of CD31+CD144+ cells by day 9 by FACS. We also looked at markers for primitive streak (T), endoderm (FOXA2) and endothelial cells (KDR, CD31 and CD144) by RT-qPCR. FACS results showed successful induction of $KDR^{+bright}$ cells in 100-3 when compared to HPAH1 (60.5% compared to 49.8% respectively), although statistical analysis was not performed in this n=1 pilot study. Both hiPSCs lines generated about 12% of CD31+CD144+ indicating that derivation of EC-like cells using our protocol may be feasible despite the presence of BMPR2 mutations (no statistical analysis was done) (figure-10 A). During the induction stage there was no apparent differences in the expression levels of all markers tested, with the possible exception of FOXA2 expression which appeared to be strong in HPAH1. By day9, there was about 10000 and 4000 folds change in the expression level of CD144 and CD31, respectively, in HPAH1-hiPSCs while about 2000 fold change in the expression level of both CD144 and CD31 in 100-3-hiPSCs (figure-10 B). Taking in consideration the limitations (comparing two different hiPSC lines from two different human beings and with different genetic backgraounds) related to this pilot experiment, the prelimenary results raise the possibility that the disturbed BMP signaling due to BMPR2 mutation could affect the induction of endothelial competent mesodermal cells, but not their specification to endothelial like cells. The second pilot experiment was designed to control for limitations in the previous experiments. Controlling for the effects of genetic background we differentiated HAPAH4-hiPSCs pre vs post correction of BMPR2. We measured the percentage of $KDR^{+bright}$ cells over the 5 induction days by FACS (Figure-10 C). These preliminary results suggest the corrected HPAH4-hiPSCs percentage of $KDR^{+bright}$ cells may be higher

than the uncorrected HPAH4-hiPSCs at each time point measured (note that no statistical analysis was performed due to the lack of replicates at each time point). This result suggests that BMPR2 mutations might affect the induction of $KDR^{+bright}$ cells or endothelial-competent mesodermal cells. The effect on generating endothelial like cells is still not investigated, and the implication that dampened BMP signaling in the BMPR2 mutant cells is responsible for this effect remains a likely possibility that requires further testing.

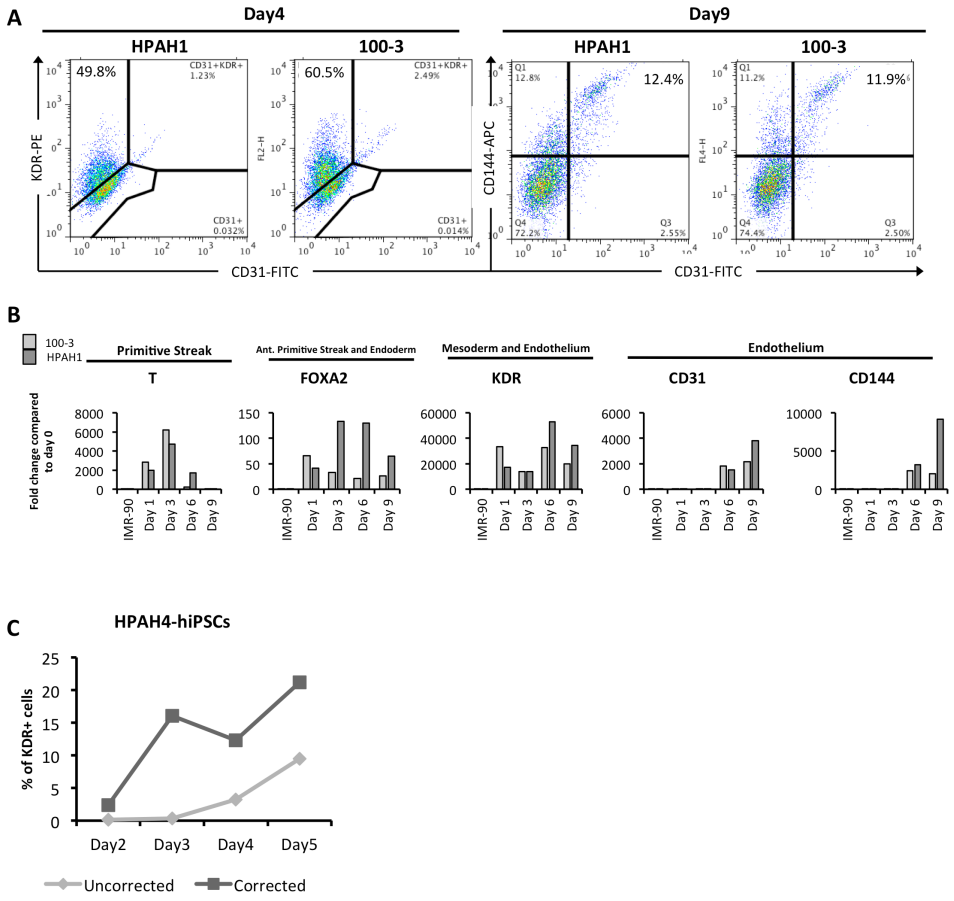

Figure 10: BMPR2 mutations potentially affect the induction of KDR+bright cells.

A. FACS plots of HPAH1-hiPSCs and 100-3-hiPSCs differentiated using media containing Activin (24hrs), BMP4, FGF2 and VEGF for 9 days.

B. Gene expression levels by RT-qPCR. Note expression levels of FOXA2 during the induction stage in HPAH1-hiPSCs when compared to 100-3-hiPSCs.

C. Line chart represent the percentage of KDR+ cells that was induced by differentiating HPAH4-hiPSCs (corrected and uncorrected). Note the consistent higher percentage of KDR+ cells generated by HPAH4-hiPSCs corrected when compared to the uncorrected line.

CHAPTER IV: DISCUSSION

We aimed in this project to develop an in vitro directed differentiation model to derive ECs from hiPSCs, which can be used for future regenerative therapies or disease models and we formulates the following hypothesis "Vascular endothelial cells can be generated in vitro from human pluripotent stem cells via the recapitulation of embryonic developmental milestones, beginning with the induction of primitive streak and mesoderm followed by specification into endothelium". To test this hypothesis, we adopted a recently published serum free, feeder free protocol (78) that used four factors (Acitivin (first 24 hrs), BMP4, VEFG and FGF) to derive ECs from hESCs and hiPSCs. The novel aspect of this published protocol, is that the authors were able to derive a population of ECs that resemble CB-ECFC in their high proliferative potential, functional vessels capabilities and maintain their phenotype in vitro for at least 18 passages without senescence or shifting to non-endothelial phenotypes. The authors called this population of ECs as iPS derived endothelial colony forming cells (iPS-ECFC). Lacking in this protocol was assessment of the kinetics of differentiation and assessment of whether the cells are going through stages that recapitulate those involved in the embryonic derivation of endothelial cells during in vivo development. During embryogenesis, ECs are derived from mesodermal cells that have been induced from posterior PS, therefore, when we tested the kinetics of the protocol, we were looking for markers that indicate the induction of primitive streak and subsequent mesodermal cells (1-4). Brachyury (T) is a pan PS marker, that has been used in many studies to trace the induction of PS (2-4,29,132). On the other hand, Flk-1 (KDR) is considered both a mesodermal and hematopoietic/endothelial progenitor marker (2-4, 29). Using these two markers, Huber et al was able to trace the induction of PS through the expression of T (using ESCs from a transgenic mouse with GFP targeted to brachyury locus) and subsequently the induction

of mesodermal cells through the expression of Flk-1. These investigators found that endothelial cells were derived only from the T+Flk1+ cells (29). Several other studies used a similar strategy to trace the derivation of endothelial cells (81,132,133). Therefore, we chose to look at the expression of T and KDR (Flk1) to test the kinetics of differentiation and to confirm the induction of PS and its transition into mesoderm. As mesoderm cells exit the PS, they are specified along the mediolateral axis into paraxial, intermediate and lateral plate mesoderm (1,2,19). Cells that form the cardiovascular system and the vasculature of all endodermal organ systems, including the lungs, are believed to be derived from the lateral plate mesoderm (1). Therefore, it was essential for us to investigate which mesodermal subsets will be induced using this differentiation protocol. Hence, we tested the kinetics of FOXF1 (lateral plate mesoderm), PAX2 (intermediate mesoderm) and TBX6 (paraxial mesoderm). Besides mesoderm, PS (specifically anterior PS) can give rise to endoderm, thus to test whether this protocol promotes endoderm formation at any stage, we used FOXA2 which is an anterior PS and endodermal marker (2,3). Finally, to trace specification into endothelial cells, we used known endothelial markers; CD31 and CD144. The results of our kinetic experiments show that over the first 4 days of the protocol, cells proceed through primitive streak stage (as revealed by the transient expression of T that peaked by day 2) and subsequently differentiate into a population of mesodermal cells that express markers of lateral plate, paraxial and intermediate mesoderm. FACS analysis at day 4 shows that about 30% of cells are $KDR^{+bright}$. With continued exposure to BMP4, VEGF and FGF for an additional 8 days, RT-qPCR results show upregulation of lateral plate mesodermal marker FOXF1 in comparison to paraxial and intermediate markers and FACS results shows a population of cells (7%) that co-expresses CD31, CD144 and KDR. When the generated CD31+CD144+KDR+ cells were sorted and replated in endothelial maintenance media,

more than 90% of cells express endothelial markers (CD31 and CD144), indicating the possibility of generating endothelial-like cells. The kinetics experiments, indicate that this in vitro differentiation protocol directed hiPSCs into PS and mesoderm stages that subsequently gave rise to endothelial-like cells, potentially replicating the process of endothelial cell derivation during development. Such transition of hiPSCs into PS and subsequently into KDR+ mesodermal cells during the first 4 days can be attributed to the induction effect of Activin and BMP4. In vivo studies indicate that Nodal and WNT signaling are essential in the formation of PS at the posterior epiblast. This was confirmed by several in vitro studies. Nostro et al found that, although BMP4 is not required for the induction of PS, the presence of BMP4 promoted posterior PS formation by day3. Evseenko et al, found that combining Activin and BMP4 with FGF2 and VEGF improved the induction of KDR+ mesodermal cells by day3.5 (134). Although this protocol favors lateral plate mesoderm over intermediate and paraxial mesoderm, which could indicate that the generated endothelial-like cells are lateral plate derived, this assumption need to be confirmed through further experiments such as lineage tracing of lateral plate mesodermal derivatives or by co-staining the day12 CD31+CD144+KDR+ with lateral plate, paraxial and intermediate mesoderm markers. On another point, there was a transient upregulation of FOXA2 that peaked by day 3 and then was downregulated for the remaining 9 days. These results indicate that this protocol did not promote endoderm formation and such transient expression of FOXA2, albeit at low levels, can be explained by transient formation of anterior PS-like phenotype in some cells. These FOXA2 levels appear to be far lower than the robust levels achieved previously in our laboratory's publications using dedicated endodermal (e.g liver, lung, or thyroid) protocols, although we have not compared these FOXA2 levels head to head in experiments in this current project.

After testing the kinetics of the protocol and generating endothelial-like cells, it was essential to characterize the generated cells and compare them to CB-ECFC using criteria described by Prasian et al (78): 1) expression and maintenance of endothelial markers 2) high proliferative potential and 3) capacity to generate functional blood vessels in vivo. The generated cells expressed endothelial markers (CD31 and CD144) and maintained that expression for at least 8 passages. They also expressed endothelial markers (CD31 and CD144), were positive to Ac-LDL update assay, and were able to form network structures in matrigel in vitro assay, all similar to CB-ECFC. When the generated $CD31^{+}CD144^{+}KDR^{+}$ cells were seeded within Matrigel plugs and transplanted subcutaneously in SCID mice they survived and formed tube-like structures that were positive for human specific anti-CD31 antibody, but failed to harbor blood cells, indicating that these tube-like structures did not anastomose with the host vascular network, and therefore may not be functional. From the kinetics and characterization assays, our data indicate that this in vitro differentiation model induces hiPSCs into stages that replicate those involved in the derivation of endothelial cells in vivo, namely formation of PS, followed by mesoderm, followed by ECs. It also yielded an endothelial like population that maintained high proliferative potential and expressed endothelial cell surface markers over several passages. Therefore, our data indicate that it is possible to use this in vitro differentiation model to investigate the factors that are involved in the induction of the different mesodermal subpopulations and their specification into endothelial cells. It can also be used to derive endothelial-like cells for regenerative models. One of the hurdles that needs to be solved is the inability of the generated ECs to form functional blood vessels in vivo. Possible explanations for this observation include our iPS-ECs assuming a developmental phenotype that may be more or less mature than CB-ECFC or contamination of our cells with fibroblastic cells either by loss of

endothelial phenotype or outgrowth of low levels of competing fibroblasts surviving our original day 12 sorts. It should be noted that mature primary ECs, in contrast to CB-ECFC, also do not exhibit functional transplantation capacity in matrigel plugs. Hence our results do not necessarily negate our interpretation that many of our iPS-EC are endothelial-ike cells even though they may differ in some ways from primary CB-ECFC.

It should be emphasized that the possibility of loss of endothelial phenotype in cultures in favor of other mesenchymal or fibroblastic phenotypes is well known. For example, it is known that endothelial cells can lose their phenotypic markers and acquire mesenchymal or myofibroblast phenotype during embryonic development, fibrotic disorders and when they cultured in vitro, in a process called endothelial to mesenchymal transition (EndoMT) (78,81,135-139). During several differentiation attempts we noticed a similar phenomena in which the sorted endothelial-like cells lost their expression of endothelial markers (CD31 and CD144) and acquired fibroblast morphology, as the number of passage increased, which indicates a possibility of EndoMT. Similar phenomena have been noticed in several published differentiation protocols. The molecular mechanism underlying EndoMT is not completely understood and is less explored compared to epithelial to mesenchymal transition. Several studies point to the role of TGF-B in causing EndoMT and its inhibition lead to the maintenance of endothelial phenotype in some studies (81,136). James et al used such a strategy of inhibiting TGF-B through the use of SB431542 during the differentiation of hiPSCs, which increased the generation of endothelial like cells by 10 fold. Continuing the inhibition of TGF-B after sorting the endothelial like cells maintained their proliferation, phenotype and resulted in a net of 36-fold expansion of endothelial cells. Using an Id1-YFP hESC reporter line, they found that the maintenance of endothelial phenotype through TGF-B inhibition is mediated through the sustained expression of Id1 (81). Their

findings support previous studies which indicate that Id1 is required for the maintenance of vascular cell fate (140). We investigated the effect of inhibiting TGF-B using SB431542 after sorting and replating $CD31^{+}CD144^{+}KDR^{+}$ cells on the maintenance of endothelial phenotype and found no significant improvement (data not shown). But we did not try the effect of TGF-B inhibition during the differentiation (specifically in the specification stage), which could possibly help in generating a more stable and perhaps more functional endothelial like population. This is a potential area for future investigation. Another possibile explanation for the lack of in vivo functional capability of our sorted $CD31^{+}CD144^{+}KDR^{+}$ cells could be related to the difference in the sorting algorithm that we used in comparison to the Prasain et al protocol. At day 12 we sorted cells according to the co-expression of three markers; CD31, CD144 and KDR. While Prasain et al (78), sorted according to the co-expression of CD31 and NRP-1 (brighter half of NRP-1 cloud on FACS plots). According to their findings, this sort gate promoted the generation of more ECFC colonies and resulted in formation of functional blood vessels in vivo in similar numbers to those formed by the positive control (CB-ECFC). They reported that with the use of their sorting algorithm they were able to purify a population of ECFC that maintained their phenotype for 18 passages without the need to use TGF-B inhibition. Interestingly, their data also revealed that even with the use of such sorting algorithm, about 50% of the sorting cells had low proliferative potential to non-dividing cells (therefore not ECFC). Similar findings were noticed with CB-ECFC. Also both CB-ECFC and hiPSC-ECFC resulted in formation of tube-like structures that did not harbor blood cells and look similar to tube-like structure that were formed by our iPS derived endothelial like cells. This indicates that their sorted cells are still not a completely pure population of ECFC. In preliminary experiments, we chose not to adopt such a sorting algorithm as we found that KDR+ cells by day 12 completely co-express

NRP-1 preventing further meaningful subgating on NRP-1 stained populations. However, we did not sort the brighter half of KDR+ cells, an approach that we might consider to investigate in an effort to increase the yield of high proliferative endothelial like cells. Another potential reason for not forming functional blood vessels in vivo could be related to the use of late passage sorted cells instead of early passage cells. As mentioned previously, we noticed that with increased numbers of passages, some cells start losing their cell surface marker expression endothelial profiles and have lower proliferative potential. Therefore before using the generated endothelial-like cells in any regenerative model, we have to address the issue of in vivo functional blood vessels forming capabilities.

HPAH is a disease of the pulmonary vasculature with 80% of reported cases carrying mutations in BMPR2 (117). While BMPR2 mutations presumably are expressed in a broad diversity of tissues and lineages, it is unknown why only the pulmonary vasculature shows clinical abnormalities. It is also unknown whether there is a developmental abnormality in the lung specific endothelial cells. Our in vitro differentiation model depends on BMP4, which is one of the ligands of BMPR2, to derive ECs from hiPSCs. Our data also indicate that this in vitro differentiation model potentially recapitulates the embryonic stages involved in the derivation of endothelial cells. Therefore it is possible to use this model to: 1) investigate the role of BMP signaling (and disturbed signaling due to mutation in BMPR2 gene) in the derivation of endothelial competent mesodermal progenitors and ECs in vitro, and 2) assist in studying the phenotype of endothelial cells generated from hiPSCs lines with mutations in BMPR2. Therefore, we first decided to investigate the role of BMP4 in different stages of the differentiation, and we designed an experiment in which BMP4 was used as the only differentiation factor during mesodermal induction (Day0-4) and/or endothelial lineage specification (Day4-12) stages of the

protocol (note that Activin was used in all conditions for the first 24hrs). Our results indicate that exposure to as little as 24 hours of exogenous BMP4 is necessary and sufficient to induce mesodermal cells with endothelial competence, and once induced, these mesodermal cells do not require BMP4 to specify to endothelial like cells. On other hand although exogenous FGF2 and VEGF exposure were not required to induce the endothelial competent mesodermal cells, they are required to specify them into endothelial like cells.

Nostro et al (133) found that Activin and WNT were sufficient and necessary for the induction of PS and FLK1+ mesodermal cells. While BMP4 was not required, but adding it promoted the derivation of posterior PS and committed mesodermal Flk1+ cells with endothelial competence. Our data shows that 24hr of BMP4 exposure was sufficient to induce the endothelial competent $KDR^{+bright}$ cells, while 24hr of Activin without exogenous source of BMP4 was not sufficient. The difference between our results and Nostro et al paper, can be attributed to the different species (Human vs mouse) and difference in differentiation setting were Nostro et al used EB based protocol, while we used monolayer based protocol. Evseenko et al (134) study, using hES model, found that significant increase in induction of $KDR^{+bright}$ cells was noticed only when BMP4, was supplemented with FGF2 and VEGF. While our data found no effect of supplementing BMP4 with VEGF or FGF2 on percentage of $KDR^{+bright}$ cells. Again the difference in the results could be attributed to the difference between EB based protocol (Evseenko et al paper) and our monolayer based protocol. To completely address whether BMP is absolutely required in our protocol in contrast to Nostro el al (133) we would need to repeat our protocol removing or blocking BMP4 in the presence of both Activin and Wnt stimulation. Thus it remains possible that as Nostro et al proposed BMP may be dispensible if downstream Wnt and TGFB/Activin signaling are stimulated during PS and

mesodermal induction. What is a common finding between Nostro et al (133), Evseenko et al (134) and our findings, is that BMP4 was not required for specifying KDR+ (Flk1+) cells into CD31 expressing cells, while VEGF is required. (keeping in mind that Evseenko et al used FBS as supplement to derive ECs from KDR+ cells). A similar finding was reported by Patsch et al (141) in which VEGF was not required for the induction of mesodermal progenitors while it is required for their specification to endothelial-like cells.

Other interesting findings in our experiments include our observation that in conditions in which 1) no factors was added or 2) combination of FGF2 and VEGF (and with Noggin) were used (with 24hr of Activin) during the induction stage, this resulted in upregulation of FOXA2 expression compared to conditions that contained BMP4. This could indicate that these conditions favored anterior primitive streak, an outcome that was suppressed by BMP4 in our studies in keeping with prior work by Keller and colleagues (2-4,132,133).

As we developed a better understanding of the role of BMP signaling in the derivation of endothelial like cells in our in vitro differentiation model, we formulated the following hypothesis "The induction of endothelial competent mesoderm is compromised in hiPSCs lines derived from patients with BMPR2 mutations resulting in insufficient derivation of endothelial-like cells". To test this hypothesis, we obtained fibroblast cells from patients having mutation in BMPR2 and affected or not with PAH. We reprogrammed the cells into hiPSCs and corrected the mutation using CRISPR/CAS9 technology (131,142). Then the corrected and uncorrected cells from the same cells line were induced for 4 days with combinations of Activin (first 24 hours), BMP4, VEGF and FGF. The results implied a lower percentage of $KDR^{+bright}$ cells in the uncorrected line over the 5 days induction time when compared to corrected line. This finding indicates a possibility of less endothelial competent mesodermal cells, but this assumption needs to be confirmed by statistical tests

on replicated results and characterizing these mesodermal cells and investigating their ability to generate endothelial like cells ($CD31^{+}CD144^{+}KDR^{+}$) by the end of the protocol. Our other preliminary and less controlled pilot experiment, in which HAPH1-hiPSCs compared to 100-3 hiPSCs showed that although there was less induction of $KDR^{+bright}$ cells by day in HPAH1-hiPSCs lines, the percentage of $CD31^{+}CD144^{+}KDR^{+}$ was similar in the two lines, indicating that the lower induction, may not affect the percentage of the endothelial like cells. Our plans to study the effect of disturbed BMP signaling due to BMPR2 mutation on the generation, phenotype and function of the endothelial like cells will continue through our collaboration with the Yoder lab at Indiana University, in which the in vivo functional blood vessel capabilities of endothelial like cells from HPAH-hiPSCs lines (corrected and uncorrected) will be tested and compared.

Through this project we were able to develop an in vitro differentiation model to derive endothelial like cells from hiPSCs via the recapitulation of embryonic developmental milestones, beginning with the induction of primitive streak and mesoderm followed by specification into endothelium. We were able to provide a better understanding of the role of BMP signaling at different stages of the differentiation, in which BMP4 was found to be necessary and sufficient to induce endothelial competent mesodermal cells, but was dispensable at the specification stages. Finally we started to use this in vitro differentiation model to develop a disease model of HPAH, by generating hiPSCs from patients with a mutation in the BMPR2 gene, correcting the mutation using CRISPR/Cas9 technology, and finally providing preliminary results on the effect of potentially disturbed BMP signaling due to BMPR2 mutation on the induction of endothelial competent mesoderm. We believe that the differentiation model can be further enhanced by optimizing it to generate endothelial like cells with in vivo functional blood vessels forming capabilities

BIBLIOGRAPHY

1. Gilbert SF. *Developmental Biology*. Evolution & Development. 2013. 10 p.

2. GADUE P, HUBER T, NOSTRO M, KATTMAN S, KELLER G. Germ layer induction from embryonic stem cells. *Experimental Hematology*. 2005;33(9): 955–964.

3. Murry CE, Keller G. Differentiation of Embryonic Stem Cells to Clinically Relevant Populations: Lessons from Embryonic Development. *Cell*. 2008;132(4): 661–680.

4. KELLER G. Embryonic stem cell differentiation: emergence of a new era in biology and medicine. *Genes & Development*. 2005;19(10): 1129–1155.

5. Liu P, Wakamiya M, Shea MJ, Albrecht U, Behringer RR, Bradley A. Requirement for Wnt3 in vertebrate axis formation. *Nature Genetics*. 1999;22(4): 361–365.

6. Varlet I, Collignon J, Robertson EJ. nodal expression in the primitive endoderm is required for specification of the anterior axis during mouse gastrulation. *Development (Cambridge, England)*. 1997;124(5): 1033–1044.

7. Conlon FL, Lyons KM, Takaesu N, Barth KS, Kispert A, Herrmann B, et al. A primary requirement for nodal in the formation and maintenance of the primitive streak in the mouse. *Development (Cambridge, England)*. 1994;120(7): 1919–1928.

8. Perea-Gomez A, Vella FDJ, Shawlot W, Oulad-Abdelghani M, Chazaud C, Meno C, et al. Nodal Antagonists in the Anterior Visceral Endoderm Prevent the Formation of Multiple Primitive Streaks. *Developmental cell*. 2002;3(5): 745–756.

9. Thomas P, Beddington R. Anterior primitive endoderm may be responsible for patterning the anterior neural plate in the mouse embryo. *Current Biology*. 1996;6(11): 1487–1496.

10. Glinka A, Wu W, Delius H, Monaghan AP, Blumenstock C, Niehrs C. Dickkopf-1 is a member of a new family of secreted proteins and functions in head induction. *Nature*. Nature Publishing Group; 1998;391(6665): 357–362.

11. Belo JA, Bachiller D, Agius E, Kemp C, Borges AC. Cerberus-like is a secreted BMP and nodal antagonist not essential for mouse development. *Genesis (New York, N.Y. : 2000)*. 2000.

12. Coucouvanis E, Martin GR. BMP signaling plays a role in visceral endoderm differentiation and cavitation in the early mouse embryo. *Development (Cambridge, England)*. The Company of Biologists Ltd; 1999;126(3): 535–546.

13. McMahon JA, Takada S, Zimmerman LB, Fan C-M, Harland RM, McMahon AP. Noggin-mediated antagonism of BMP signaling is required for growth and patterning of the neural tube and somite. *Genes & Development*. Cold Spring Harbor Lab; 1998;12(10): 1438–1452.

14. Lawson KA, Dunn NR, Roelen BA, Zeinstra LM, Davis AM, Wright CV, et al. Bmp4 is required for the generation of primordial germ cells in the mouse embryo. *Genes & Development*. Cold Spring Harbor Lab; 1999;13(4): 424–436.

15. Bachiller D, Klingensmith J, Kemp C, Belo JA, Anderson RM, May SR, et al. The organizer factors Chordin and Noggin are required for mouse forebrain development. *Nature*. Nature Publishing Group; 2000;403(6770): 658–661.

16. Tonegawa A, Funayama N, Ueno N, Takahashi Y. Mesodermal subdivision along the mediolateral axis in chicken controlled by different concentrations of BMP-4. *Development (Cambridge, England)*. The Company of Biologists Ltd; 1997;124(10): 1975–1984.

17. Pourquié O, Fan C-M, Coltey M, Hirsinger E, Watanabe Y, Bréant C, et al. Lateral and Axial Signals Involved in Avian Somite Patterning: A Role for BMP4. *Cell*. 1996;84(3): 461–471.

18. Wilm B, James RG, Schultheiss TM, Hogan BLM. The forkhead genes, Foxc1 and Foxc2, regulate paraxial versus intermediate mesoderm cell fate. *Developmental biology*. 2004;271(1): 176–189.

19. Mahlapuu M, Ormestad M, Enerbäck S, Carlsson P. The forkhead transcription factor Foxf1 is required for differentiation of extra-embryonic and lateral plate mesoderm. *Development (Cambridge, England)*. 2001;128(2): 155–166.

20. Dumont DJ, Fong GH, Puri MC, Gradwohl G, Alitalo K, Breitman ML. Vascularization of the mouse embryo: a study of flk-1, tek, tie, and vascular endothelial growth factor expression during development. *Developmental dynamics : an official publication of the American Association of Anatomists*. Wiley Subscription Services, Inc., A Wiley Company; 1995;203(1): 80–92.

21. Ema M, Takahashi S, Rossant J. Deletion of the selection cassette, but not cis-acting elements, in targeted Flk1-lacZ allele reveals Flk1 expression in multipotent mesodermal progenitors. *Blood*. American Society of Hematology; 2006;107(1): 111–117.

22. Shalaby F, Rossant J, Yamaguchi TP, Gertsenstein M, Wu X-F, Breitman ML, et al. Failure of blood-island formation and vasculogenesis in Flk-1-deficient mice. *Nature*. Nature Publishing Group; 1995;376(6535): 62–66.

23. Lee D, Park C, Lee H, Lugus JJ, Kim SH, Arentson E, et al. ER71 acts downstream of BMP, Notch, and Wnt signaling in blood and vessel progenitor specification. *Cell stem cell*. 2008;2(5): 497–507.

24. Ema M, Faloon P, Zhang WJ, Hirashima M, Reid T, Stanford WL, et al. Combinatorial effects of Flk1 and Tal1 on vascular and hematopoietic development in the mouse. *Genes & Development*. Cold Spring Harbor Lab;

2003;17(3): 380–393.

25. Fehling HJ, Lacaud G, Kubo A, Kennedy M, Robertson S, Keller G, et al. Tracking mesoderm induction and its specification to the hemangioblast during embryonic stem cell differentiation. *Development (Cambridge, England)*. 2003;130(17): 4217–4227.

26. Chung YS, Zhang WJ, Arentson E, Kingsley PD, Palis J, Choi K. Lineage analysis of the hemangioblast as defined by FLK1 and SCL expression. *Development (Cambridge, England)*. 2002;129(23): 5511–5520.

27. Motoike T, Markham DW, Rossant J, Sato TN. Evidence for novel fate of Flk1+ progenitor: contribution to muscle lineage. *Genesis (New York, N.Y. : 2000)*. Wiley Subscription Services, Inc., A Wiley Company; 2003;35(3): 153–159.

28. Faloon P, Arentson E, Kazarov A, Deng CX, Porcher C, Orkin S, et al. Basic fibroblast growth factor positively regulates hematopoietic development. *Development (Cambridge, England)*. 2000;127(9): 1931–1941.

29. Huber TL, Kouskoff V, Fehling HJ, Palis J, Keller G. Haemangioblast commitment is initiated in the primitive streak of the mouse embryo. *Nature*. 2004;432(7017): 625–630.

30. Breier G, Clauss M, Risau W. Coordinate expression of vascular endothelial growth factor receptor-1 (flt-1) and its ligand suggests a paracrine regulation of murine vascular development. *Developmental dynamics : an official publication of the American Association of Anatomists*. Wiley Subscription Services, Inc., A Wiley Company; 1995;204(3): 228–239.

31. Breier G, Albrecht U, Sterrer S, Risau W. Expression of vascular endothelial growth factor during embryonic angiogenesis and endothelial cell differentiation. *Development (Cambridge, England)*. 1992;114(2): 521–532.

32. Carmeliet P, Ferreira V, Breier G, Pollefeyt S, Kieckens L, Gertsenstein M, et al. Abnormal blood vessel development and lethality in embryos lacking a single VEGF allele. *Nature*. 1996;380(6573): 435–439.

33. Deng CX, Wynshaw-Boris A, Shen MM, Daugherty C, Ornitz DM, Leder P. Murine FGFR-1 is required for early postimplantation growth and axial organization. *Genes & Development*. Cold Spring Harbor Lab; 1994;8(24): 3045–3057.

34. Xu X, Weinstein M, Li C, Naski M, Cohen RI, Ornitz DM, et al. Fibroblast growth factor receptor 2 (FGFR2)-mediated reciprocal regulation loop between FGF8 and FGF10 is essential for limb induction. *Development (Cambridge, England)*. The Company of Biologists Ltd; 1998;125(4): 753–765.

35. Lee SH, Schloss DJ, Swain JL. Maintenance of vascular integrity in the embryo requires signaling through the fibroblast growth factor receptor. *Journal of Biological Chemistry*. American Society for Biochemistry and Molecular Biology; 2000;275(43): 33679–33687.

36. Sabin FR. *Preliminary note on the differentiation of angioblasts and the method by which they produce blood-vessels, blood-plasma and red blood-cells as seen in the living chick. 1917.* Journal of hematotherapy & stem cell research. 2002. 3 p.

37. Murray P. The Development in vitro of the Blood of the Early Chick Embryo on JSTOR. 1932.

38. Manaia A, Lemarchandel V, Klaine M, Max-Audit I, Romeo P, Dieterlen-Lievre F, et al. Lmo2 and GATA-3 associated expression in intraembryonic hemogenic sites. *Development (Cambridge, England)*. The Company of Biologists Ltd; 2000;127(3): 643–653.

39. Takakura N, Huang X-L, Naruse T, Hamaguchi I, Dumont DJ, Yancopoulos GD, et al. Critical Role of the TIE2 Endothelial Cell Receptor in the Development of Definitive Hematopoiesis. *Immunity*. 1998;9(5): 677–686.

40. Garcia-Porrero JA, Manaia A, Jimeno J, Lasky LL, Dieterlen-Lièvre F, Godin IE. Antigenic profiles of endothelial and hemopoietic lineages in murine intraembryonic hemogenic sites. *Developmental & Comparative Immunology*. 1998;22(3): 303–319.

41. Wood HB, May G, Healy L, Enver T, Morriss-Kay GM. CD34 Expression Patterns During Early Mouse Development Are Related to Modes of Blood Vessel Formation and Reveal Additional Sites of Hematopoiesis. *Blood*. American Society of Hematology; 1997;90(6): 2300–2311.

42. Marshall CJ, Thrasher AJ. The embryonic origins of human haematopoiesis. *British journal of haematology*. Blackwell Science Ltd; 2001;112(4): 838–850.

43. Vogeli KM, Jin S-W, Martin GR, Stainier DYR. A common progenitor for haematopoietic and endothelial lineages in the zebrafish gastrula. *Nature*. Nature Publishing Group; 2006;443(7109): 337–339.

44. Ferkowicz MJ, Yoder MC. Blood island formation: longstanding observations and modern interpretations. *Experimental Hematology*. 2005;33(9): 1041–1047.

45. Ueno H, Weissman IL. The origin and fate of yolk sac hematopoiesis: application of chimera analyses to developmental studies. *The International journal of developmental biology*. UPV/EHU Press; 2010;54(6-7): 1019–1031.

46. Padrón-Barthe L, Temiño S, del Campo CV, Carramolino L, Isern J, Torres M. Clonal analysis identifies hemogenic endothelium as the source of the blood-endothelial common lineage in the mouse embryo. *Blood*. American Society of Hematology; 2014;124(16): 2523–2532.

47. Eilken HM, Nishikawa S-I, Schroeder T. Continuous single-cell imaging of blood generation from haemogenic endothelium. *Nature*. Nature Publishing Group; 2009;457(7231): 896–900.

48. Sugiyama D, Ogawa M, Hirose I, Jaffredo T, Arai K-I, Tsuji K. Erythropoiesis from acetyl LDL incorporating endothelial cells at the preliver stage. *Blood*.

American Society of Hematology; 2003;101(12): 4733–4738.

49. Lancrin C, Sroczynska P, Stephenson C, Allen T, Kouskoff V, Lacaud G. The haemangioblast generates haematopoietic cells through a haemogenic endothelium stage. *Nature*. Nature Publishing Group; 2009;457(7231): 892–895.

50. Chen MJ, Yokomizo T, Zeigler BM, Dzierzak E, Speck NA. Runx1 is required for the endothelial to haematopoietic cell transition but not thereafter. *Nature*. Nature Publishing Group; 2009;457(7231): 887–891.

51. Evans MJ, Kaufman MH. Establishment in culture of pluripotential cells from mouse embryos. *Nature*. Nature Publishing Group; 1981;292(5819): 154–156.

52. Martin GR. Isolation of a pluripotent cell line from early mouse embryos cultured in medium conditioned by teratocarcinoma stem cells. *Proceedings of the National Academy of Sciences*. National Acad Sciences; 1981;78(12): 7634–7638.

53. Thomson JA, Itskovitz-Eldor J, Shapiro SS, Waknitz MA, Swiergiel JJ, Marshall VS, et al. Embryonic stem cell lines derived from human blastocysts. *Science (New York, N.Y.)*. 1998;282(5391): 1145–1147.

54. GURDON JB. The developmental capacity of nuclei taken from intestinal epithelium cells of feeding tadpoles. *Journal of embryology and experimental morphology*. 1962;10: 622–640.

55. Tada M, Takahama Y, Abe K, Nakatsuji N, Tada T. Nuclear reprogramming of somatic cells by in vitro hybridization with ES cells. *Current biology : CB*. 2001;11(19): 1553–1558.

56. Schneuwly S, Klemenz R, Gehring WJ. Redesigning the body plan of Drosophila by ectopic expression of the homoeotic gene Antennapedia. *Nature*. 1987;325(6107): 816–818.

57. Davis RL, Weintraub H, Lassar AB. Expression of a single transfected cDNA converts fibroblasts to myoblasts. *Cell*. 1987;51(6): 987–1000.

58. Takahashi K, Yamanaka S. Induction of Pluripotent Stem Cells from Mouse Embryonic and Adult Fibroblast Cultures by Defined Factors. *Cell*. 2006;126(4): 663–676.

59. Takahashi K, Tanabe K, Ohnuki M, Narita M, Ichisaka T, Tomoda K, et al. Induction of pluripotent stem cells from adult human fibroblasts by defined factors. *Cell*. 2007;131(5): 861–872.

60. Yu J, Vodyanik MA, Smuga-Otto K, Antosiewicz-Bourget J, Frane JL, Tian S, et al. Induced pluripotent stem cell lines derived from human somatic cells. *Science (New York, N.Y.)*. American Association for the Advancement of Science; 2007;318(5858): 1917–1920.

61. Yamanaka S. Induced Pluripotent Stem Cells: Past, Present, and Future. *Cell stem cell*. 2012;10(6): 678–684.

62. Takahashi K, Yamanaka S. A decade of transcription factor-mediated reprogramming to pluripotency. *Nature reviews. Molecular cell biology*. 2016;17(3): 183–193.

63. Sommer CA, Stadtfeld M, Murphy GJ, Hochedlinger K, Kotton DN, Mostoslavsky G. Induced pluripotent stem cell generation using a single lentiviral stem cell cassette. *Stem cells (Dayton, Ohio)*. Wiley Subscription Services, Inc., A Wiley Company; 2009;27(3): 543–549.

64. Somers A, Jean J-C, Sommer CA, Omari A, Ford CC, Mills JA, et al. Generation of transgene-free lung disease-specific human induced pluripotent stem cells using a single excisable lentiviral stem cell cassette. *Stem cells (Dayton, Ohio)*. Wiley Subscription Services, Inc., A Wiley Company; 2010;28(10): 1728–1740.

65. Sommer CA, Sommer AG, Longmire TA, Christodoulou C, Thomas DD, Gostissa M, et al. Excision of reprogramming transgenes improves the differentiation potential of iPS cells generated with a single excisable vector. *Stem cells (Dayton, Ohio)*. Wiley Subscription Services, Inc., A Wiley Company; 2010;28(1): 64–74.

66. Stadtfeld M, Nagaya M, Utikal J, Weir G, Hochedlinger K. Induced pluripotent stem cells generated without viral integration. *Science (New York, N.Y.)*. American Association for the Advancement of Science; 2008;322(5903): 945–949.

67. Zhou W, Freed CR. Adenoviral gene delivery can reprogram human fibroblasts to induced pluripotent stem cells. *Stem cells (Dayton, Ohio)*. Wiley Subscription Services, Inc., A Wiley Company; 2009;27(11): 2667–2674.

68. Seki T, Yuasa S, Oda M, Egashira T, Yae K, Kusumoto D, et al. Generation of induced pluripotent stem cells from human terminally differentiated circulating T cells. *Cell stem cell*. 2010;7(1): 11–14.

69. Fusaki N, Ban H, Nishiyama A, Saeki K, Hasegawa M. Efficient induction of transgene-free human pluripotent stem cells using a vector based on Sendai virus, an RNA virus that does not integrate into the host genome. *Proceedings of the Japan Academy. Series B, Physical and biological sciences*. 2009;85(8): 348–362.

70. Warren L, Manos PD, Ahfeldt T, Loh Y-H, Li H, Lau F, et al. Highly efficient reprogramming to pluripotency and directed differentiation of human cells with synthetic modified mRNA. *Cell stem cell*. Elsevier; 2010;7(5): 618–630.

71. Woltjen K, Michael IP, Mohseni P, Desai R, Mileikovsky M, Hämäläinen R, et al. piggyBac transposition reprograms fibroblasts to induced pluripotent stem cells. *Nature*. 2009;458(7239): 766–770.

72. Narsinh KH, Jia F, Robbins RC, Kay MA, Longaker MT, Wu JC. Generation of adult human induced pluripotent stem cells using nonviral minicircle DNA vectors. *Nature protocols*. 2011;6(1): 78–88.

73. Okita K, Nakagawa M, Hyenjong H, Ichisaka T, Yamanaka S. Generation of

mouse induced pluripotent stem cells without viral vectors. *Science (New York, N.Y.)*. American Association for the Advancement of Science; 2008;322(5903): 949–953.

74. Archer S. Measurement of nitric oxide in biological models. *FASEB journal : official publication of the Federation of American Societies for Experimental Biology*. 1993;7(2): 349–360.

75. Tatsumi R, Suzuki Y, Sumi T, Sone M, Suemori H, Nakatsuji N. Simple and highly efficient method for production of endothelial cells from human embryonic stem cells. *Cell transplantation*. Cognizant Communication Corporation; 2011;20(9): 1423–1430.

76. Tognarelli S, Gayet J, Lambert M, Dupuy S, Karras A, Cohen P, et al. Tissue-specific microvascular endothelial cells show distinct capacity to activate NK cells: implications for the pathophysiology of granulomatosis with polyangiitis. *Journal of immunology (Baltimore, Md. : 1950)*. American Association of Immunologists; 2014;192(7): 3399–3408.

77. Rufaihah AJ, Huang NF, Jamé S, Lee JC, Nguyen HN, Byers B, et al. Endothelial cells derived from human iPSCS increase capillary density and improve perfusion in a mouse model of peripheral arterial disease. *Arteriosclerosis, thrombosis, and vascular biology*. American Heart Association, Inc; 2011;31(11): e72–e79.

78. Prasain N, Lee MR, Vemula S, Meador JL, Yoshimoto M, Ferkowicz MJ, et al. Differentiation of human pluripotent stem cells to cells similar to cord-blood endothelial colony-forming cells. *Nature biotechnology*. Nature Research; 2014;32(11): 1151–1157.

79. Levenberg S, Golub JS, Amit M, Itskovitz-Eldor J, Langer R. Endothelial cells derived from human embryonic stem cells. *Proceedings of the National Academy of Sciences*. National Acad Sciences; 2002;99(7): 4391–4396.

80. Yu J, Huang NF, Wilson KD, Velotta JB, Huang M, Li Z, et al. nAChRs mediate human embryonic stem cell-derived endothelial cells: proliferation, apoptosis, and angiogenesis. Linden R (ed.) *PloS one*. Public Library of Science; 2009;4(9): e7040.

81. James D, Nam H-S, Seandel M, Nolan D, Janovitz T, Tomishima M, et al. Expansion and maintenance of human embryonic stem cell-derived endothelial cells by TGFbeta inhibition is Id1 dependent. *Nature biotechnology*. Nature Research; 2010;28(2): 161–166.

82. White MP, Rufaihah AJ, Liu L, Ghebremariam YT, Ivey KN, Cooke JP, et al. Limited gene expression variation in human embryonic stem cell and induced pluripotent stem cell-derived endothelial cells. *Stem cells (Dayton, Ohio)*. Wiley Subscription Services, Inc., A Wiley Company; 2013;31(1): 92–103.

83. Vodyanik MA, Thomson JA, Slukvin II. Leukosialin (CD43) defines hematopoietic progenitors in human embryonic stem cell differentiation cultures.

Blood. American Society of Hematology; 2006;108(6): 2095–2105.

84. Choi K-D, Yu J, Smuga-Otto K, Salvagiotto G, Rehrauer W, Vodyanik M, et al. Hematopoietic and endothelial differentiation of human induced pluripotent stem cells. *Stem cells (Dayton, Ohio)*. Wiley Subscription Services, Inc., A Wiley Company; 2009;27(3): 559–567.

85. Wang ZZ, Au P, Chen T, Shao Y, Daheron LM, Bai H, et al. Endothelial cells derived from human embryonic stem cells form durable blood vessels in vivo. *Nature biotechnology*. Nature Publishing Group; 2007;25(3): 317–318.

86. Sahara M, Hansson EM, Wernet O, Lui KO, Später D, Chien KR. Manipulation of a VEGF-Notch signaling circuit drives formation of functional vascular endothelial progenitors from human pluripotent stem cells. *Cell research*. 2014;24(7): 820–841.

87. Tuder RM, Abman SH, Braun T, Capron F, Stevens T, Thistlethwaite PA, et al. Development and pathology of pulmonary hypertension. *Journal of the American College of Cardiology*. 2009;54(1 Suppl): S3–S9.

88. Thompson K, Rabinovitch M. Exogenous leukocyte and endogenous elastases can mediate mitogenic activity in pulmonary artery smooth muscle cells by release of extracellular-matrix bound basic fibroblast growth factor. *Journal of cellular physiology*. Wiley Subscription Services, Inc., A Wiley Company; 1996;166(3): 495–505.

89. Alastalo T-P, Li M, Perez V de J, Pham D, Sawada H, Wang JK, et al. Disruption of PPARγ/β-catenin-mediated regulation of apelin impairs BMP-induced mouse and human pulmonary arterial EC survival. *The Journal of clinical investigation*. American Society for Clinical Investigation; 2011;121(9): 3735–3746.

90. Xu W, Kaneko FT, Zheng S, Comhair SAA, Janocha AJ, Goggans T, et al. Increased arginase II and decreased NO synthesis in endothelial cells of patients with pulmonary arterial hypertension. *FASEB journal : official publication of the Federation of American Societies for Experimental Biology*. Federation of American Societies for Experimental Biology; 2004;18(14): 1746–1748.

91. Passman JN, Dong XR, Wu S-P, Maguire CT, Hogan KA, Bautch VL, et al. A sonic hedgehog signaling domain in the arterial adventitia supports resident Sca1+ smooth muscle progenitor cells. *Proceedings of the National Academy of Sciences of the United States of America*. National Acad Sciences; 2008;105(27): 9349–9354.

92. Davie NJ, Crossno JT, Frid MG, Hofmeister SE, Reeves JT, Hyde DM, et al. Hypoxia-induced pulmonary artery adventitial remodeling and neovascularization: contribution of progenitor cells. *American journal of physiology. Lung cellular and molecular physiology*. American Physiological Society; 2004;286(4): L668–L678.

93. Frid MG, Kale VA, Stenmark KR. Mature vascular endothelium can give rise to smooth muscle cells via endothelial-mesenchymal transdifferentiation: in vitro

analysis. *Circulation Research*. 2002;90(11): 1189–1196.

94. Sakao S, Tatsumi K, Voelkel NF. Endothelial cells and pulmonary arterial hypertension: apoptosis, proliferation, interaction and transdifferentiation. *Respiratory research*. BioMed Central; 2009;10(1): 95.

95. Taraseviciene-Stewart L, Gera L, Hirth P, Voelkel NF, Tuder RM, Stewart JM. A bradykinin antagonist and a caspase inhibitor prevent severe pulmonary hypertension in a rat model. *Canadian journal of physiology and pharmacology*. 2002;80(4): 269–274.

96. Masri FA, Xu W, Comhair SAA, Asosingh K, Koo M, Vasanji A, et al. Hyperproliferative apoptosis-resistant endothelial cells in idiopathic pulmonary arterial hypertension. *American journal of physiology. Lung cellular and molecular physiology*. American Physiological Society; 2007;293(3): L548–L554.

97. Runo JR, Loyd JE. Primary pulmonary hypertension. *Lancet (London, England)*. 2003;361(9368): 1533–1544.

98. Simonneau G, Gatzoulis MA, Adatia I, Celermajer D, Denton C, Ghofrani A, et al. Updated clinical classification of pulmonary hypertension. *Journal of the American College of Cardiology*. 2013;62(25 Suppl): D34–D41.

99. Rich S, Dantzker DR, Ayres SM, Bergofsky EH, Brundage BH, Detre KM, et al. Primary pulmonary hypertension. A national prospective study. *Annals of internal medicine*. 1987;107(2): 216–223.

100. Nichols WC, Koller DL, Slovis B, Foroud T. Localization of the gene for familial primary pulmonary hypertension to chromosome 2q31-32. *Nature*. 1997.

101. Morse JH, Barst RJ. Detection of familial primary pulmonary hypertension by genetic testing. *The New England journal of medicine*. 1997;337(3): 202–203.

102. Lane KB, Machado RD, Pauciulo MW, Thomson JR, Phillips JA, Loyd JE, et al. Heterozygous germline mutations in BMPR2, encoding a TGF-|[beta]| receptor, cause familial primary pulmonary hypertension. *Nature Genetics*. Nature Publishing Group; 2000;26(1): 81–84.

103. Deng Z, Morse JH, Slager SL, Cuervo N, Moore KJ, Venetos G, et al. Familial Primary Pulmonary Hypertension (Gene PPH1) Is Caused by Mutations in the Bone Morphogenetic Protein Receptor–II Gene. *The American Journal of Human Genetics*. 2000;67(3): 737–744.

104. Newman JH, Wheeler L, Lane KB, Loyd E, Gaddipati R, Phillips JA, et al. Mutation in the gene for bone morphogenetic protein receptor II as a cause of primary pulmonary hypertension in a large kindred. *The New England journal of medicine*. 2001;345(5): 319–324.

105. Loyd JE, Primm RK, Newman JH. Familial primary pulmonary hypertension: clinical patterns. *The American review of respiratory disease*. 1984;129(1): 194–197.

106. Loyd JE, Slovis B, Phillips JA, Butler MG, Foroud TM, Conneally PM, et al. The presence of genetic anticipation suggests that the molecular basis of familial primary pulmonary hypertension may be trinucleotide repeat expansion. *Chest*. 1997;111(6 Suppl): 82S–83S.

107. Miyazono K, Maeda S, Imamura T. BMP receptor signaling: transcriptional targets, regulation of signals, and signaling cross-talk. *Cytokine & growth factor reviews*. 2005;16(3): 251–263.

108. Kawabata M, Imamura T, Miyazono K. Signal transduction by bone morphogenetic proteins. *Cytokine & growth factor reviews*. 1998;9(1): 49–61.

109. Massagué J, Chen YG. Controlling TGF-beta signaling. *Genes & Development*. 2000;14(6): 627–644.

110. Attisano L, Wrana JL. Signal transduction by the TGF-beta superfamily. *Science (New York, N.Y.)*. American Association for the Advancement of Science; 2002;296(5573): 1646–1647.

111. Rosenzweig BL, Imamura T, Okadome T, Cox GN, Yamashita H, Dijke ten P, et al. Cloning and characterization of a human type II receptor for bone morphogenetic proteins. *Proceedings of the National Academy of Sciences*. National Academy of Sciences; 1995;92(17): 7632–7636.

112. Nickel J, Kotzsch A, Sebald W, Mueller TD. A single residue of GDF-5 defines binding specificity to BMP receptor IB. *Journal of molecular biology*. 2005;349(5): 933–947.

113. Massagué J, Seoane J, Wotton D. Smad transcription factors. *Genes & Development*. Cold Spring Harbor Lab; 2005;19(23): 2783–2810.

114. Thomson JR, Machado RD, Pauciulo MW, Morgan NV, Humbert M, Elliott GC, et al. Sporadic primary pulmonary hypertension is associated with germline mutations of the gene encoding BMPR-II, a receptor member of the TGF-beta family. *Journal of medical genetics*. BMJ Group; 2000;37(10): 741–745.

115. Machado RD, Eickelberg O, Elliott CG, Geraci MW, Hanaoka M, Loyd JE, et al. Genetics and genomics of pulmonary arterial hypertension. *Journal of the American College of Cardiology*. 2009;54(1 Suppl): S32–S42.

116. Machado RD, Aldred MA, James V, Harrison RE, Patel B, Schwalbe EC, et al. Mutations of the TGF-beta type II receptor BMPR2 in pulmonary arterial hypertension. *Human mutation*. Wiley Subscription Services, Inc., A Wiley Company; 2006;27(2): 121–132.

117. Morrell NW. Pulmonary hypertension due to BMPR2 mutation: a new paradigm for tissue remodeling? *Proceedings of the American Thoracic Society*. 2006;3(8): 680–686.

118. Rudarakanchana N, Flanagan JA, Chen H, Upton PD, Machado R, Patel D, et al. Functional analysis of bone morphogenetic protein type II receptor mutations underlying primary pulmonary hypertension. *Human molecular genetics*.

2002;11(13): 1517–1525.

119. Sobolewski A, Rudarakanchana N, Upton PD, Yang J, Crilley TK, Trembath RC, et al. Failure of bone morphogenetic protein receptor trafficking in pulmonary arterial hypertension: potential for rescue. *Human molecular genetics*. Oxford University Press; 2008;17(20): 3180–3190.

120. Long L, MacLean MR, Jeffery TK, Morecroft I, Yang X, Rudarakanchana N, et al. Serotonin increases susceptibility to pulmonary hypertension in BMPR2-deficient mice. *Circulation Research*. American Heart Association, Inc; 2006;98(6): 818–827.

121. Yu PB, Beppu H, Kawai N, Li E, Bloch KD. Bone morphogenetic protein (BMP) type II receptor deletion reveals BMP ligand-specific gain of signaling in pulmonary artery smooth muscle cells. *Journal of Biological Chemistry*. American Society for Biochemistry and Molecular Biology; 2005;280(26): 24443–24450.

122. Valdimarsdottir G, Goumans M-J, Rosendahl A, Brugman M, Itoh S, Lebrin F, et al. Stimulation of Id1 Expression by Bone Morphogenetic Protein Is Sufficient and Necessary for Bone Morphogenetic Protein–Induced Activation of Endothelial Cells. *Circulation*. American Heart Association, Inc; 2002;106(17): 2263–2270.

123. Teichert-Kuliszewska K, Kutryk MJB, Kuliszewski MA, Karoubi G, Courtman DW, Zucco L, et al. Bone Morphogenetic Protein Receptor-2 Signaling Promotes Pulmonary Arterial Endothelial Cell Survival. *Circulation Research*. American Heart Association, Inc; 2006;98(2): 209–217.

124. Yang X, Long L, Southwood M, Rudarakanchana N, Upton PD, Jeffery TK, et al. Dysfunctional Smad Signaling Contributes to Abnormal Smooth Muscle Cell Proliferation in Familial Pulmonary Arterial Hypertension. *Circulation Research*. American Heart Association, Inc; 2005;96(10): 1053–1063.

125. McDonald PP, Fadok VA, Bratton D, Henson PM. Transcriptional and translational regulation of inflammatory mediator production by endogenous TGF-beta in macrophages that have ingested apoptotic cells. *Journal of immunology (Baltimore, Md. : 1950)*. 1999;163(11): 6164–6172.

126. Wang D, Prakash J, Nguyen P, Davis-Dusenbery BN, Hill NS, Layne MD, et al. Bone morphogenetic protein signaling in vascular disease: anti-inflammatory action through myocardin-related transcription factor A. *Journal of Biological Chemistry*. American Society for Biochemistry and Molecular Biology; 2012;287(33): 28067–28077.

127. Davies RJ, Holmes AM, Deighton J, Long L, Yang X, Barker L, et al. BMP type II receptor deficiency confers resistance to growth inhibition by TGF-β in pulmonary artery smooth muscle cells: role of proinflammatory cytokines. *American journal of physiology. Lung cellular and molecular physiology*. American Physiological Society; 2012;302(6): L604–L615.

128. Burton VJ, Holmes AM, Ciuclan LI, Robinson A, Roger JS, Jarai G, et al. Attenuation of leukocyte recruitment via CXCR1/2 inhibition stops the progression of PAH in mice with genetic ablation of endothelial BMPR-II. *Blood*. American Society of Hematology; 2011;118(17): 4750–4758.

129. Burton VJ, Ciuclan LI, Holmes AM, Rodman DM, Walker C, Budd DC. Bone morphogenetic protein receptor II regulates pulmonary artery endothelial cell barrier function. *Blood*. American Society of Hematology; 2011;117(1): 333–341.

130. Chevalier F, Lavergne M, Negroni E, Ferratge S, Carpentier G, Gilbert-Sirieix M, et al. Glycosaminoglycan mimetic improves enrichment and cell functions of human endothelial progenitor cell colonies. *Stem cell research*. 2014;12(3): 703–715.

131. Ran FA, Hsu PD, Wright J, Agarwala V, Scott DA, Zhang F. Genome engineering using the CRISPR-Cas9 system. *Nature protocols*. Nature Research; 2013;8(11): 2281–2308. Available from: doi:10.1038/nprot.2013.143

132. Gadue P, Huber TL, Paddison PJ, Keller GM. Wnt and TGF-beta signaling are required for the induction of an in vitro model of primitive streak formation using embryonic stem cells. *Proceedings of the National Academy of Sciences*. National Acad Sciences; 2006;103(45): 16806–16811.

133. Nostro MC, Cheng X, Keller GM, Gadue P. Wnt, Activin, and BMP Signaling Regulate Distinct Stages in the Developmental Pathway from Embryonic Stem Cells to Blood. *Cell stem cell*. 2008;2(1): 60–71.

134. Evseenko D, Zhu Y, Schenke-Layland K, Kuo J, Latour B, Ge S, et al. Mapping the first stages of mesoderm commitment during differentiation of human embryonic stem cells. *Proceedings of the National Academy of Sciences of the United States of America*. National Acad Sciences; 2010;107(31): 13742–13747.

135. Arciniegas E, Neves CY, Carrillo LM, Zambrano EA, Ramírez R. Endothelial-mesenchymal transition occurs during embryonic pulmonary artery development. *Endothelium : journal of endothelial cell research*. 2005;12(4): 193–200.

136. Goumans M-J, van Zonneveld AJ, Dijke ten P. Transforming Growth Factor β–Induced Endothelial-to-Mesenchymal Transition: A Switch to Cardiac Fibrosis? *Trends in Cardiovascular Medicine*. 2008;18(8): 293–298.

137. Hashimoto N, Phan SH, Imaizumi K, Matsuo M, Nakashima H, Kawabe T, et al. Endothelial–Mesenchymal Transition in Bleomycin-Induced Pulmonary Fibrosis. *American Journal of Respiratory Cell and Molecular Biology*. American Thoracic Society; 2012;43(2): 161–172.

138. Zeisberg EM, Potenta SE, Sugimoto H, Zeisberg M, Kalluri R. Fibroblasts in Kidney Fibrosis Emerge via Endothelial-to-Mesenchymal Transition. *Journal of the American Society of Nephrology*. American Society of Nephrology; 2008;19(12): 2282–2287.

139. Zeisberg EM, Tarnavski O, Zeisberg M, Dorfman AL, McMullen JR, Gustafsson

E, et al. Endothelial-to-mesenchymal transition contributes to cardiac fibrosis. *Nature Medicine*. Nature Publishing Group; 2007;13(8): 952–961.

140. Ruzinova MB, Benezra R. Id proteins in development, cell cycle and cancer. *Trends in cell biology*. 2003;13(8): 410–418.

141. Patsch C, Challet-Meylan L, Thoma EC, Urich E, Heckel T, O'Sullivan JF, et al. Generation of vascular endothelial and smooth muscle cells from human pluripotent stem cells. *Nature cell biology*. 2015;17(8): 994–1003.

142. Wright AV, Nuñez JK, Doudna JA. Biology and Applications of CRISPR Systems: Harnessing Nature's Toolbox for Genome Engineering. *Cell*. 2016;164(1-2): 29–44.

CURRICULUM VITAE